Impact of Climatic Changes on Downstream Hydraulic Geometry and its Influence on Flood Hydrograph Routing – Applied to the Bluestone Dam Watershed

---

PLAN B TECHNICAL REPORT

SUMMER 2015

Prepared By:

Nicholas A. Koutsunis

Advised By:

Dr. Pierre Y. Julien

IN PARTIAL FULFILLMENT OF THE REQUIREMENTS
FOR MASTER OF SCIENCE DEGREE – PLAN B

Colorado State University
Department of Civil and Environmental Engineering
Fort Collins, Colorado 80523

Acknowledgements

This research was completed at Colorado State University as part of the Master's of Science in Hydraulic Engineering program advised by Dr. Pierre Julien, funded by the U.S. Army Corps of Engineers.

Abstract

There have been three previous Inflow Design Flood (IDF) studies within the Bluestone Watershed. The Bluestone Dam Original IDF Study resulted in a peak inflow of 430,000 cfs and the 1982 Bluestone Dam IDF Study, based on the definition of the Probable Maximum Flood (PMF) prescribed in USACE guidance, resulted in a peak inflow of 1,086,000 cfs. The 2014 Bluestone Dam IDF Study resulted in a peak inflow of 1,466,100 cfs. Comparison from 1982 to the 2014 Bluestone Dam IDF Study showed that the hydrologic routing of discharge from each subbasin through the watershed is a key component of the analysis. The Muskingum-Cunge physically based routing method was used for the 2014 study. As has been documented and researched for many years, rivers are a dynamic system that is constantly changing to reach an equilibrium between driving and resisting forces. The most important contributor to a river's behavior is the climate. This study analyzes the potential changes in downstream hydraulic geometry as a result of increased discharge due to climate change. To perform this analysis, changes to channel geometry were applied to the Bluestone Dam watershed.

The analysis was conducted by first developing downstream hydraulic geometry relative relationship curves based on the Julien-Wargadalam (J-W) equations. The dominant discharge for nine (9) gaged locations in the watershed was determined through statistical analysis. The downstream hydraulic geometry dimensions were then calculated and verified to existing models and areal imagery. The downstream hydraulic geometry changes were then applied to the Muskingum-Cunge hydrologic routing method to determine impacts to flood hydrograph routing. Completion of these objectives then allowed for comparison to be made between dominant discharge and flood hydrograph routing for three scenarios: current conditions, 100-percent and 500-percent increase in dominant discharge.

Results indicate that for the Bluestone Dam watershed, an increase in dominant discharge 100% would decrease the attenuation and increase the peak discharge approximately 3.1%. An increase in dominant discharge 500% would further decrease the attenuation and increase the peak discharge approximately 6.4%. These results show that flood wave attenuation decreases as the dominant discharge increases. However, due to the relatively small percentage difference in results, and with consideration of the other uncertainties involved with the development of an IDF, the impact of climate change on the routing of extreme flood events in the Bluestone Dam watershed is not considered a driving factor in terms of hydrograph development.

Table of Contents

List of Tables

Table of Figures

Chapter 1
Introduction

There have been three previous Inflow Design Flood (IDF) studies within the Bluestone Watershed. The Bluestone Dam Original IDF Study resulted in a peak inflow of 430,000 cfs and the 1982 Bluestone Dam IDF Study, based on the definition of the Probable Maximum Flood (PMF) prescribed in the U.S. Army Corps of Engineers (USACE) guidance, resulted in a peak inflow of 1,086,000 cfs. The 2014 Bluestone Dam IDF Study resulted in a peak inflow of approximately 1,400,000 cfs. A brief description of the Bluestone Dam Original Inflow Design Flood, the 1982 Bluestone Dam IDF Study and the 2014 Bluestone Dam IDF Study are presented in the subsequent sections of this chapter.

1.1 Bluestone Dam Original IDF

The Bluestone Dam Original Inflow Design Flood was calculated by the USACE - Huntington District prior to construction of the dam. The original hydrologic design criteria for Bluestone Lake was based on historical records that were available at that time. The original inflow design flood was derived from a hurricane type storm that occurred in July 1916 near Altapass, NC. The center of the storm was transposed to a location within the New River Basin where the physiographic characteristics were similar to those at the actual storm center.

The resulting inflow hydrograph had a peak discharge of 430,000 cfs. The flood was routed through the project with an assumed initial lake level at the flood control elevation of 1520 feet (NGVD 1929). The resulting stage hydrograph had a peak lake elevation of 1523 feet (NGVD 1929).

1.2 1982 Bluestone Dam IDF Study

The 1982 Bluestone Dam IDF Study was conducted by the Huntington District Corps of Engineers and the National Weather Service as part of the Dam Safety Assurance Program. The PMP was determined through a site specific study conducted by the Hydrometeorological branch of the National Weather Service. This site-specific study was conducted because the Bluestone Watershed falls within the stippled region of the National Weather Service's HMR 51 report. Estimates within the stippled area are recommended for site-specific studies due to the anticipated effects that elevation and orography would impose on the PMP values from HMR 51. The resulting basin average precipitation estimates for the Bluestone Watershed was computed to be approximately 20 inches.

The Snyder Synthetic Unit Hydrograph parameters were determined based on the characteristics of the watershed. The watershed was divided into 15 sub-basins. The gaged sub-basins were calibrated to one of three storms; June 1949, December 1950, or March 1943 storm event. The runoff parameters developed from the gaged sub-basins were transferred to the ungaged sub-basins using the Snyder Transfer Method.

The 1982 Bluestone Dam IDF Study concluded that the PMP (20 inches) applied to the watershed would produce a peak inflow of 1,086,000 cfs at the dam site.

1.3 2014 Bluestone Dam IDF Study

The 2014 Bluestone Dam IDF Study was conducted by the Huntington District Corps of Engineers as part of the Dam Safety Assurance Program. The PMP developed for the 1982 study was revised by the USACE Extreme Storm Team. The updated PMP was reduced by 10% to a basin average precipitation of 18 inches. The hydrologic model was also updated based on an additional 30 years of hourly stream flow data and resulted in a more hydraulically efficient model than used in previous studies. The 2014 Bluestone Dam IDF Study concluded that the averaged PMP (18 inches) applied to the watershed would produce a peak inflow of 1,466,100 cfs at the dam site.

1.4 Climate Considerations for Hydrologic Routing

Comparison from 1982 to the 2014 Bluestone Dam IDF Study showed that the hydrologic routing of discharge from each subbasin through the watershed is a key component of the analysis. The Muskingum-Cunge physically based routing method was used for the 2014 study. As has been documented and researched for many years, rivers are a dynamic system that is constantly changing to reach an equilibrium between driving and resisting forces. The most important contributor to a river's behavior is the climate. This study aims to describe potential impacts to the routing of large floods through a watershed caused by climate change.

1.4.1 Climate Outlook

Precipitation has increased, on average, approximately five (5) percent over the past 50 years, as shown in Figure 1. Future precipitation projections indicate that the northern United States will continue to become wetter while the southern areas, mainly in the West, will become drier (Karl et. al., 2009). This study is focused on the impacts of increased precipitation to river hydraulics and does not focus on any implications with regards to drier conditions.

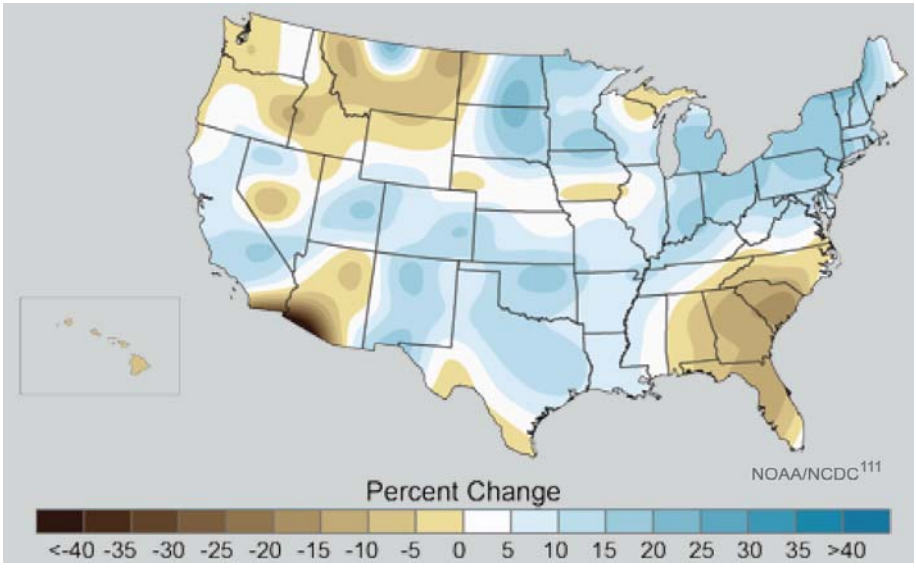

Figure 1. Observed Change in Annual Average Precipitation from 1958-2008 (from Karl et. al., 2009).

Fluvial systems are sensitive to the magnitude and frequency of large storm events and extreme floods are expected to increase due to a warmer climate (Lettenmaier et. al., 2008). There are clear trends showing that heavy precipitation, defined as the heaviest 1 percent of all daily precipitation events, is increasing for the entire United States, as shown in Figure 2.

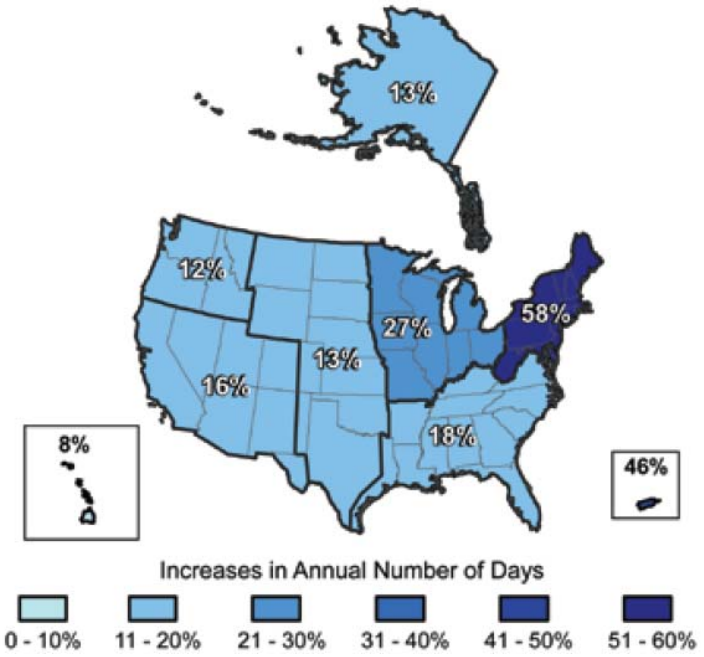

Figure 2. Increase in Number of Days with Very Heavy Precipitation from 1958 to 2007 (from Karl et. al., 2009).

The runoff from large storm events is a function of the timing and intensity of the precipitation, among other considerations such as soil moisture and interception. As the world warms, wetter and drier conditions will prevail as regional and seasonal precipitation patterns change. This will cause rainfall to become more concentrated into heavy events with longer dry period in between (Karl et. al., 2009). The frequency and intensity of extreme precipitation events is expected to increase for the entire United States. This will result in an increase of runoff, as illustrated in Figure 3.

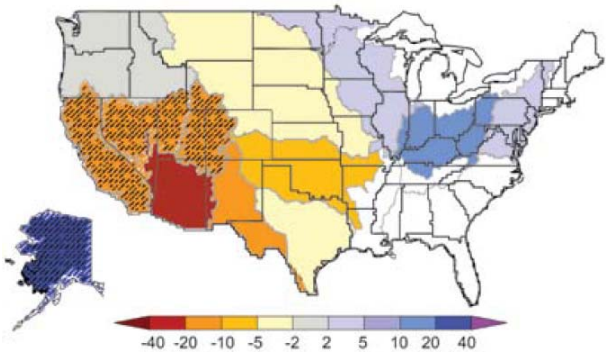

Figure 3. Projected percent change in median runoff for 2041-2060, relative to a 1901-1970 baseline. Hatched area shows high confidence. White area shows model divergence. (from Lettenmaier et. al., 2008)

As runoff is expected to increase due to the climate changing, rivers will attempt to reach a new equilibrium that accounts for the increased discharge. The volume and

timing of the discharge is therefore directly determined by climatic forces and their influence not only on precipitation but also the upstream watershed geometry (hillslopes and valley-channel network) and material characteristics (Flores, 2006)

Alluvial rivers have the ability to deform its own boundary to migrate laterally while at the same time changing their longitudinal profile. This morphology can be described as either 1) at-a-station hydraulic geometry, and 2) downstream hydraulic geometry. The at-a-station hydraulic geometry considers a fixed cross-section to define the relationship between river width, depth, velocity, and slope as a function of discharge. This relationship assumes mean flow conditions and is not used to describe the river geometry based on flood conditions. The downstream hydraulic geometry, based on bankfull river conditions, allows for an understanding of river morphology in the downstream direction as a function of discharge (Julien, 2015).

1.5 Study Objectives

This study aims to analyze the potential changes in downstream hydraulic geometry as a result of increased discharge due to climate change. To perform this analysis, three main objectives were defined as:

- Develop relative relationships between an increase in dominant discharge and the resulting impacts to downstream hydraulic geometry.
- Calculate and verify the downstream hydraulic geometry dimensions for gaged locations within the Bluestone Dam watershed
- Apply downstream hydraulic geometry changes to the Muskingum-Cunge hydrologic routing method to determine impacts to flood hydrograph routing.

Completion of these objectives then allowed for comparison to be made between dominant discharge and flood hydrograph routing for three scenarios: current conditions, 100-percent and 500-percent increase in dominant discharge.

Chapter 2
Watershed Characteristics

2.1 Location Description

Bluestone Lake Dam is located in Southeast West Virginia on the New River, approximately three (3) miles above the city of Hinton, WV. The drainage area of the dam is approximately 4,620 square miles located in the Upper New River (HUC 05050001) and Middle New River (HUC 05050002) watersheds. The watershed extends from the south near Boone, North Carolina, north through the western panhandle of Virginia and into southern West Virginia. The location of the watershed is shown in Figure 4.

The reservoir at full pool covers portions of Summers, Monroe, and Mercer Counties in West Virginia and a portion of Giles County in Virginia. The dam is a concrete gravity structure with a gated spillway located in the channel section of the dam along with outlet works through the spillway section. Six (6) penstocks are located in the right abutment, which have been modified to provide additional discharge capacity during an extreme storm event.

Major flooding in the basin can occur at any time of the year. Summer rains are often generated by thunderstorm activity, which typically occurs over small areas and produces high intensity rainfalls over a short period of time. The basin is also prone to larger tropical systems that can produce large rainfall depths over large areas. Precipitation from late fall to early spring is generally associated with the passage of low pressure systems over the basin. If these systems become stationary or move slowly, prolonged precipitation is possible. These types of systems can produce flooding conditions over large areas.

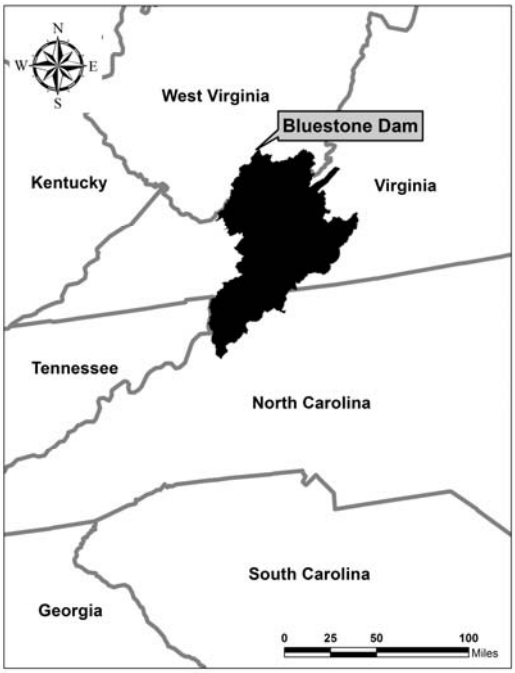

Figure 4. Location map of Bluestone Dam watershed

2.1.1 Topography and Vegetation

The New River watershed lies in a mountainous region of the Allegheny Plateau, a region which has been deeply dissected by the New, Greenbrier and Bluestone Rivers. Valleys are deep and narrow, the flood plain being only slightly wider than the river channel, which varies in width from 100 to 1,000 feet. In many places, the banks are sheer bluffs rising from the edge of the river. Elevations range from 1,370 feet (NGVD29) near the Bluestone Lake dam to 5,723 feet (NGVD29) at Mount Rogers on the western slope of the Allegheny Mountains. The land use of the study area is shown in Figure 5. The majority of the watershed is characterized by forested areas with some concentrated areas of pasture land. There are few developed locations in the watershed.

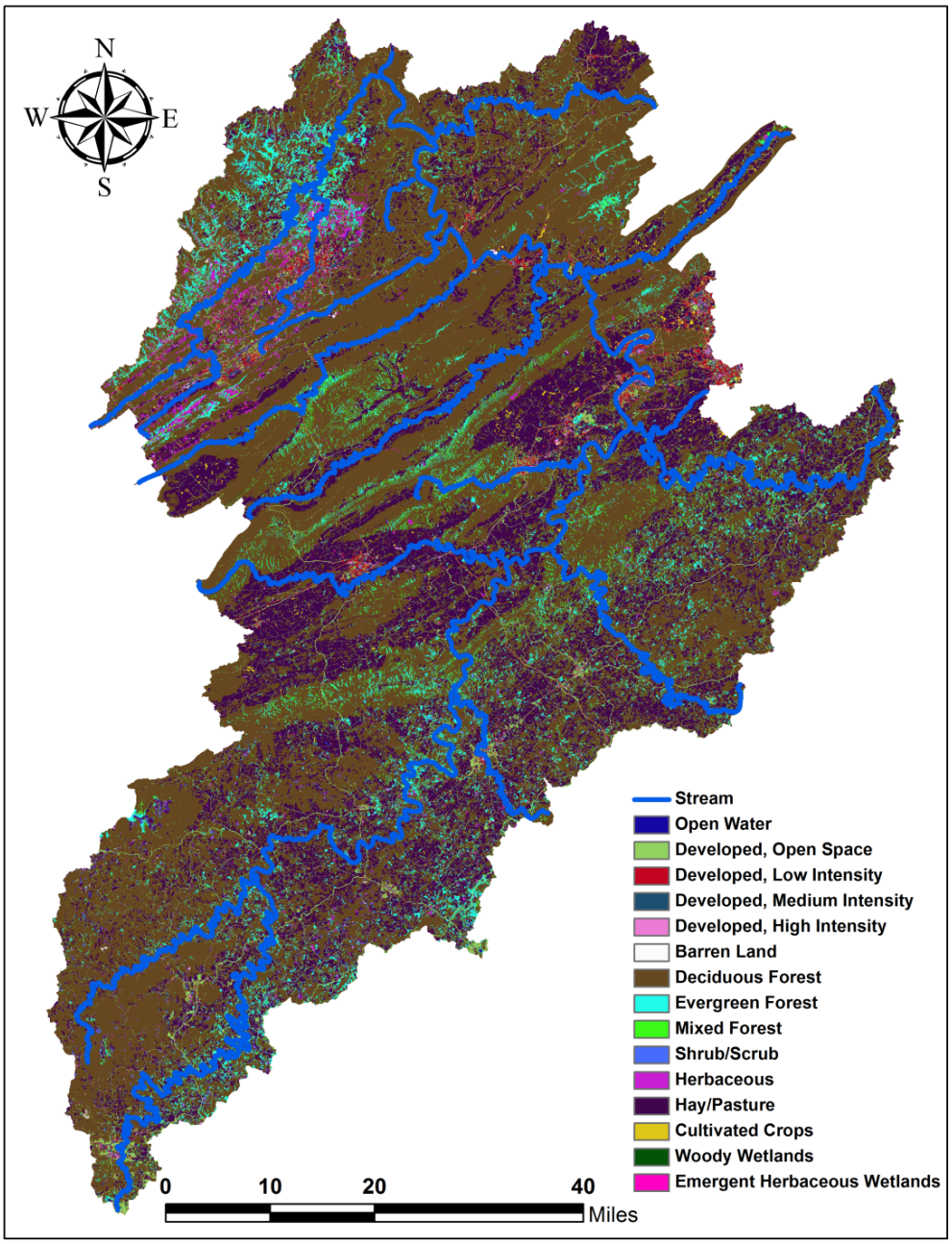

Figure 5. Land-use classification for Bluestone Dam watershed

Bluestone watershed is described by three physiographic regions (Figure 6) that have distinct runoff characteristics. The Appalachian Plateau is the western part of the Appalachian Mountains, stretching from New York to Alabama. The surface of the plateau slopes gently to the northwest and merges into the Interior Plains. The Valley and Ridge region are part of the Appalachian division and forms a broad arc between the Blue Ridge Mountains and the Appalachian Plateau physiographic region. The Blue Ridge region marks the western boundary of the watershed and features the steepest terrain prone to high intensity rainfall capable of producing flash floods.

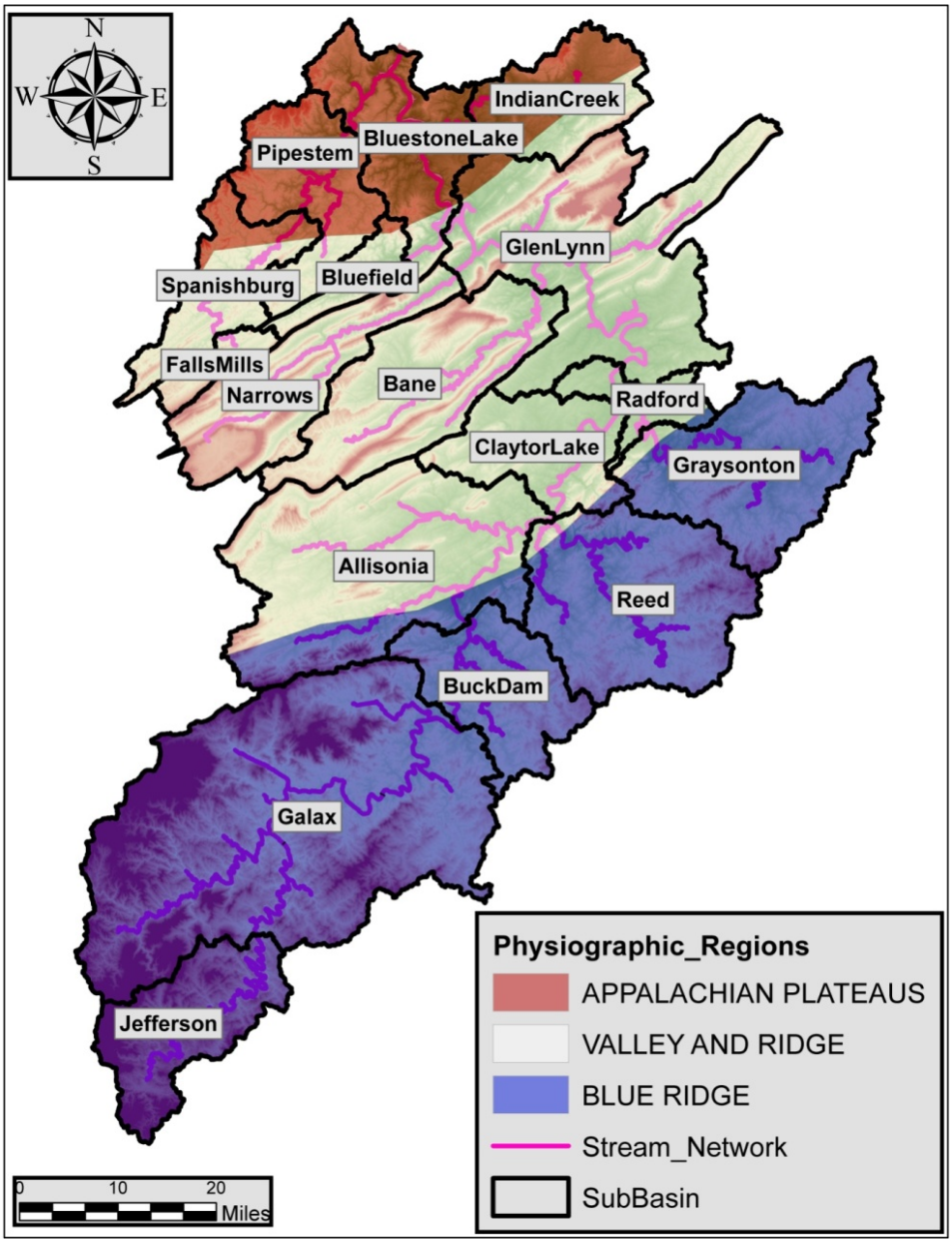

Figure 6. Physiographic regions within the Bluestone Dam watershed

2.1.2 Precipitation and Snowfall

Precipitation within the Bluestone Watershed is heavily influenced by topography. Normal annual precipitation for the watershed ranges 37 to 50 inches with a large portion of the watershed averaging 40 to 44 inches annually. Normal monthly rainfall ranges from 2.4 inches in February near Wytheville, VA (approx. elevation 2,300 feet, NGVD29) to five (5) inches in March near Banner Elk, NC (approx. elevation 3,700 feet, NGVD29). Seasonal snowfall ranges from 19.8 inches at Wytheville, Virginia to 45.9 inches at Banner Elk, North Carolina.

2.1.3 Rivers and Tributaries

The New River has its sources in the Blue Ridge Mountains of northwestern North Carolina near the Tennessee border. The river flows northeasterly into Virginia to near Radford, where it turns abruptly and flows northwesterly into West Virginia to Bluestone Lake. Throughout almost its entire course, the river flows through rugged, mountainous country. Ledges of limestone, sandstone and shale cross the river at frequent intervals, creating rapids and waterfalls. The stream is steep, having an average slope of 9.2 feet per mile in its length of 341 miles. Bluestone Lake is located in the section having the flattest slope, 4.2 feet per mile.

Chapter 3
Data and Methods

3.1 Data

The data used in this analysis was provided from the United States Geologic Survey (USGS) and U.S. Army Corps of Engineers (USACE).

3.1.1 Existing Models

The USACE Hydrologic Engineering Center's Hydrologic Modeling System (HEC-HMS) was used for the 2014 Bluestone Dam Inflow Design Flood Update model and was employed for this analysis. A schematic showing the subbasin delineation is shown in Figure 7, with the general direction of flow being south to north. This model has been calibrated to three large storm events and validated to the basin flood of record. This analysis is focused on the hydrologic routing of large floods through the watershed and only the applicable data/information to this study will be presented and discussed.

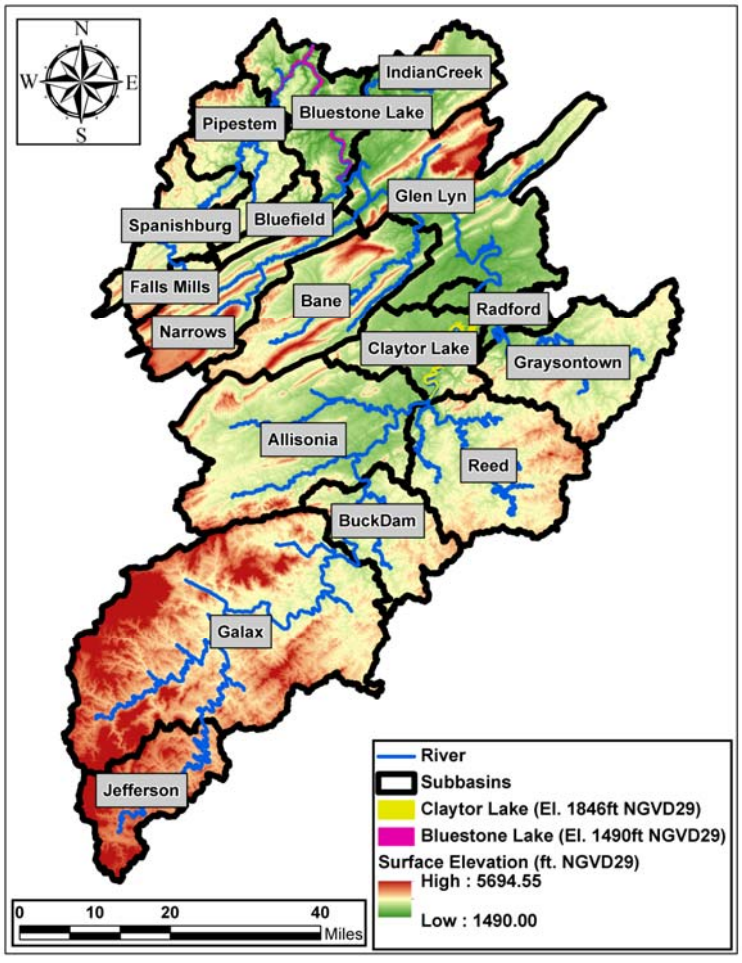

Figure 7. Subbasin delineation used for hydrologic modeling using HEC-HMS

3.1.1.1 Methodology

The Hydrologic Engineering Center's Hydrologic Modeling System (HEC-HMS) was used to perform the rainfall-runoff computations. This model was selected based on its widespread use, flexibility, and use in the existing forecast model for water management of the Kanawha River Basin. Initial parameter estimates were made using GIS data and previous analysis, including the daily operational forecast model. Model parameters were refined through calibration by comparing model results to historic flow measurements. The Snyder Transfer Method was used to characterize the rainfall-runoff relationship of the un-gaged sub-basins within the watershed through transferring the Snyder Synthetic Unit Hydrograph parameters from gaged sub-basins. The model was validated to a historic event by comparing model results (using the model developed during calibration) to historic flow measurements. Once the calibration and validation was complete, the model was modified to account for higher intensity rainfall resulting from the PMP; in accordance with USACE guidelines.

3.1.1.2 Development of the HEC-HMS Model

A HEC-HMS model has three main components: basin model, meteorologic model, and control specifications. HEC-HMS contains multiple methods for modeling the transformation of precipitation to runoff at the sub-basin outlet, baseflow, and the movement of water from an upstream location to a downstream location (i.e. channel routing). A summary of the equations and required parameters for each method are included in the HEC-HMS Technical Reference Manual (HEC, 2000). Table 1 contains modeling methods chosen and a list of required parameters.

Table 1. HEC-HMS modeling methods and required parameters

Modeling Method	Parameter	Description
Initial and Constant Loss Method	Initial Loss (inches)	Initial loss parameter that accounts for the moisture condition in the watershed at the beginning of the simulation – loss from canopy interception, surface storage, and infiltration.
	Constant Loss Rate (inches/hour)	Infiltration rate during saturated soil conditions.
	Percent Impervious Area	Impervious area directly connected to the channel network (no losses are computed).
Snyder Synthetic Unit Hydrograph Parameters	Standard Lag (hours)	The time from the center of mass of excess rainfall to the hydrograph peak.
	Peaking Coefficient	Dimensionless parameter affecting hydrograph shape.
Recession Baseflow	Initial Discharge per Area (cfs/mi^2)	Initial baseflow at the beginning of the simulation
	Recession Constant	Parameter used to control how fast the recession hydrograph trends to 0 cfs.
	Ratio to Peak	Parameter used to control when baseflow is "turned on"

		during a flood event. This parameter tells the program to start the baseflow recession once the receding limb of the direct runoff hydrograph reaches a certain threshold (the threshold is computed using the ratio of the flow to the peak flow).
Muskingum-Cunge Routing Method	Physical Basin Parameters	Reach Length (ft); Slope (ft/ft); Manning's n-values; 8-point Cross-Section

The following list provides a general overview of the steps followed for developing the HMS model, calibrating and validating it to historical events, and finally modeling the IDF event. These steps are discussed in more detail in the following sections.

1. **Sub-basin delineation and initial parameter estimates.** The delineation of this model was based on GIS data to delineate sub-basin and river reaches in the study area. Locations of sub-basin delineation were chosen based on the availability of stream flow data and to create the largest area that still can still be reasonably "lumped" into one set of watershed variables that explain the response. Parameters for this study were initially estimated using GIS data, previous study results, and the water management forecast model.

2. **HEC-HMS model calibration and validation.** The HEC-HMS model was calibrated to historic rainfall-runoff events. Model parameters were adjusted (within reasonable limits) until the model was able to reproduce, as accurately as possible, observed peak flows and volume. The calibrated model was then applied to an additional historic event to validate the model.

3. **Simulation of the IDF event using a modified version of the calibrated HEC-HMS model.** Precipitation data for the PMP event was developed during a site-specific study dated April 2014. The PMP was input into the calibrated HEC-HMS model to determine the IDF into Bluestone Dam.

3.1.1.3 Routing Reach Parameterization Calibration

Routing of sub-basin hydrographs within a watershed is necessary to be able to capture the attenuation of flow while moving downstream through the channel and floodplain. In the hydrologic model, this is performed using routing reaches. In order to thoroughly examine the routing parameters for the Bluestone Dam watershed, a detailed analysis was conducted using hydrologic routings, steady flow hydraulic analysis, and unsteady flow hydraulic routings.

The Muskingum-Cunge hydrologic routing method was employed for the main river reaches throughout the Bluestone Dam watershed. This method was chosen based on the need for a routing method capable of properly calculating discharge through a routing reach for a wide range of flow conditions, up to the IDF discharges, far beyond the largest calibration event. A HEC-RAS steady flow hydraulic model was used to validate the Muskingum-Cunge routing parameters used in the HEC-HMS hydrologic model at three gaged locations along the main stem of the New River within the Bluestone Dam watershed. The gages used for this analysis are located in Table 2.

Table 2. Stream flow gages used for HEC-RAS model calibration

Gage	Latitude	Longitude	USGS ID	Drainage Area (sq. mi.)	Gage Datum (feet, NGVD29)
Galax, VA	36.6472 N	80.9792 W	03164000	1,141	2,208.04
Radford, VA	37.1417 N	80.5694 W	03171000	2,951	1,712.16
Glen Lyn, VA	37.3728 N	80.8608 W	03168000	3,966	1,490.11

The three individual steady flow hydraulic models were developed and calibrated to the published USGS rating curves at each respective location. Upon completion of calibration, the inflow hydrograph peak discharges at each gage, calculated within the HEC-HMS model, were input into the steady hydraulic model to determine an average cross-sectional velocity. This was then compared to the average reach velocities calculated using the Muskingum-Cunge hydrologic routing method by determining an average reach routing based on reach length and attenuation of the hydrograph peak discharge. Comparisons of velocities are listed in

Table 3 and show that the Muskingum-Cunge hydrologic routing method is able to accurately estimate discharges throughout the basin.

Table 3. Comparison of velocities (ft/s) computed using HEC-RAS and HEC-HMS for the calibration events

	Galax, VA			Radford, VA			Glen Lyn, VA		
Event	Flow (kcfs)	RAS (ft/s)	HMS (ft/s)	Flow (kcfs)	RAS (ft/s)	HMS (ft/s)	Flow (kcfs)	RAS (ft/s)	HMS (ft/s)
January 1995 Calibration	68	6.4	7.5	119	5.7	5.8	131	8.9	9.5
March 2010 Calibration	15	4.8	4.7	40	4.0	4.3	62	8.0	8.1
March 2011 Calibration	20	5.1	5.2	50	4.3	4.5	63	8.1	8.0
August 1940 Validation	140	7.0	8.2	180	6.4	6.7	226	9.6	11.0

Note: The August 1940 event data was developed from discharge gages outside the basin. The values tested for this portion of the analysis represent the values from the calibrated hydrologic model.

The comparison of velocities for the calibration events is possible due to the majority of discharge being routed downstream through the channel. However, for the IDF, significant out-of-bank discharge is expected to occur based on the physical characteristics of the New River. Activation of storage within the overbank areas during the IDF could influence attenuation of discharge through the river reach. This consideration was the basis for choosing the Muskingum-Cunge routing method for use in the hydrologic routing model.

In order to adequately validate the hydrologic routing for events with discharges on the scale of the IDF, further analysis was conducted using hydraulic routing. An unsteady flow HEC-RAS hydraulic model was constructed along the 62 mile reach (Figure 8) between the Galax, VA gage and Allisonia, VA gage in the headwaters of the watershed, upstream of Claytor Lake Dam. This location was chosen for further analysis based on the length of this reach, data availability and quality of data needed for proper calibration. The unsteady flow HEC-RAS hydraulic model was constructed using the best available Digital Elevation Model (10-meter) for the entire reach. A channel was estimated using aerial photography and a FEMA Flood Insurance Study, where available. The study reach was then calibrated to two major flood events along this reach; January, 1995 and September, 1989.

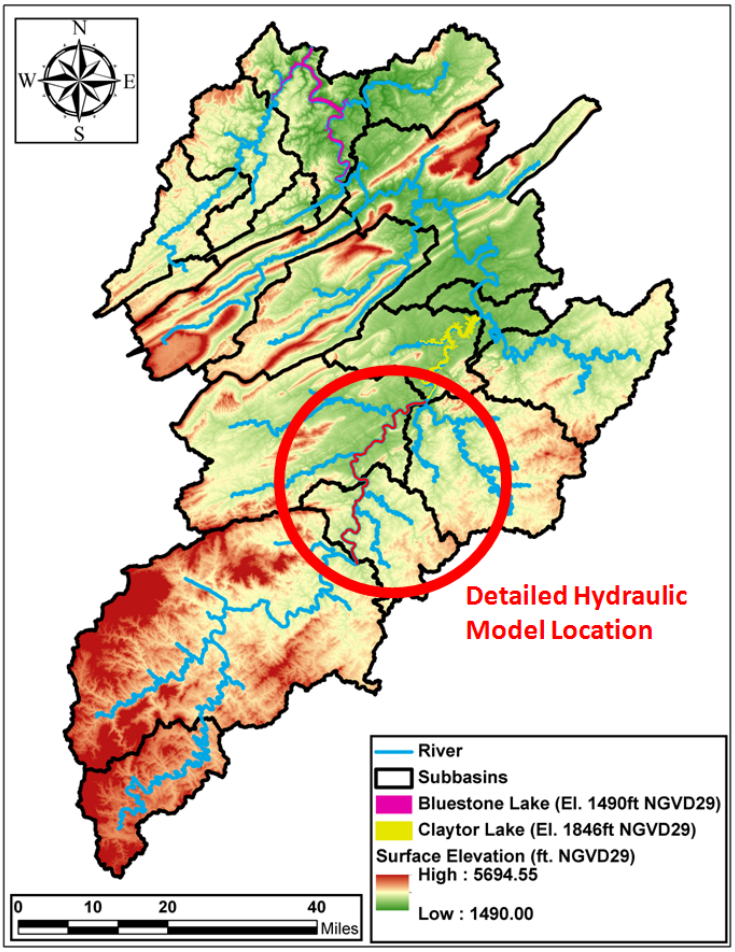

Figure 8. Location map of detailed HEC-RAS hydraulic model used for routing parameter validation

The IDF was routed through the calibrated HEC-RAS unsteady flow model and produced results comparable to the Muskingum-Cunge hydrologic routing in the HEC-HMS model. The results of the attenuation through the 62 mile river reach are listed for both hydrologic (Muskingum-Cunge) and hydraulic (unsteady flow HEC-RAS) routing methods in Table 4, and compared graphically in Figure 9.

Table 4. Routing method attenuation comparison

Routing Method	Time Attenuation (hours)	Peak Inflow (cfs)	Absolute Peak Reach Outflow (cfs)
Muskingum-Cunge (HMS)	3.00	676,600	669,000
Unsteady Flow Hydraulic Model (RAS)	3.25		651,300

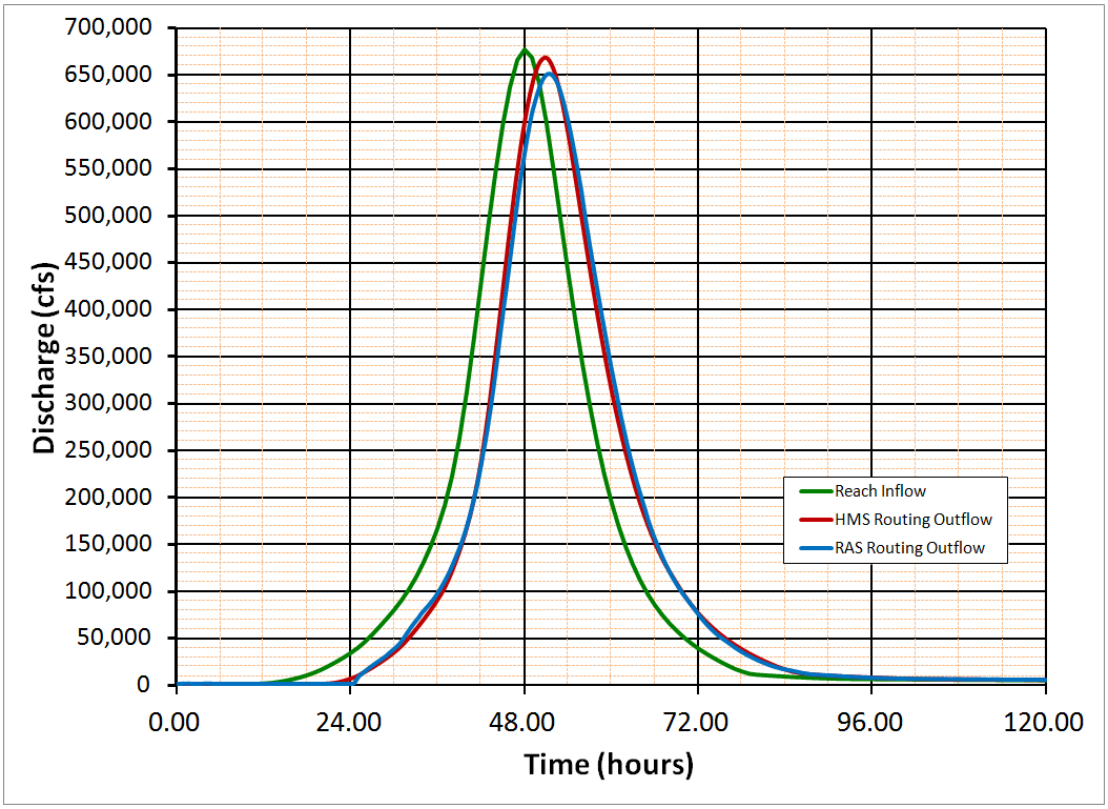

Figure 9. Reach routing attenuation comparison

The increase in attenuation calculated by the HEC-RAS hydraulic model could be explained on the ability of the model to account for storage in tributaries along the study reach that are activated during large storm events. With consideration given to the other input parameters and uncertainties within the study, the performance of the Muskingum-Cunge routing parameters to estimate large discharges through a reach, as expected during the IDF event, is considered to be acceptable and applicable. The adopted routing parameters used for this study are listed in Table 5.

Table 5. Muskingum-Cunge routing parameters used for hydrologic modeling

			Manning's n-values		
Reach	**Length (feet)**	**Slope (ft/ft)**	**Channel**	**Overbank**	**Cross-Section Type**
Jefferson to Galax	376,119	0.0040	0.045	0.075	8-Point
Galax to Buck Dam	93,235	0.0021	0.045	0.075	8-Point
Buck Dam to Allisonia	116,316	0.0017	0.045	0.075	8-Point
Claytor Lake to RRP	2,882	0.0015	0.05	0.085	8-Point
RRP to Radford	46,235	0.0017	0.05	0.085	8-Point
Graysontown to RRP	25,160	0.0015	0.05	0.085	8-Point
Radford to Walker Creek	191,388	0.0014	0.05	0.085	8-Point
Walker Creek	43,009	0.0021	0.03	0.07	8-Point
Walker Creek to Wolf Creek	65,752	0.0012	0.03	0.07	8-Point
Wolf Creek	18,524	0.0038	0.03	0.07	8-Point
Wolf Creek to Glen Lyn	34,016	0.0010	0.03	0.07	8-Point
Glen Lyn to East River	1,846	0.0010	0.03	0.07	8-Point
East River	38,779	0.0048	0.03	0.07	8-Point
Falls Mills to Spansihburg	169,462	0.0060	0.045	0.075	8-Point
Spanishburg to Pipestem	124,385	0.0042	0.045	0.075	8-Point

3.1.1.4 Model Calibration to Historic Events

Model calibration is the process of adjusting model parameters, within reasonable physical limits, to reflect watershed conditions in order to reproduce historic flow events. Model parameters were adjusted to minimize the difference in computed and measured flow at the USGS gage locations shown in Figure 11 and listed in

Three storm events were used to calibrate the model. Because the goal of this study was to model an extreme rainfall-runoff event, it was important to calibrate to the largest historical events on record, considering observed data time step and data integrity. The historic events chosen for model calibration included the January 1995, March 2010 and March 2011 events. These storm events were selected primarily for two reasons; 1) because they produced high peak discharges at the gaged subbasins, and 2) because they produced high peak discharges at Bluestone Dam. Consideration was also given to other contributing factors that can impact a rainfall-runoff analysis, such as snow melt. Research of historical documents provided by the National Climatic Data Center ensured that all calibration events carried forward in determining the IDF were not impacted by snow melt. Other events produced higher peak discharges at Bluestone Dam, as can be seen Figure 10. However, significantly high unit discharges were not recorded at any gaged sub-basins upstream of the dam during these events. This suggests that runoff characteristics of this watershed, likely influenced by the mountainous topography,

are capable of producing isolated runoff events that produce large inflows into the dam.

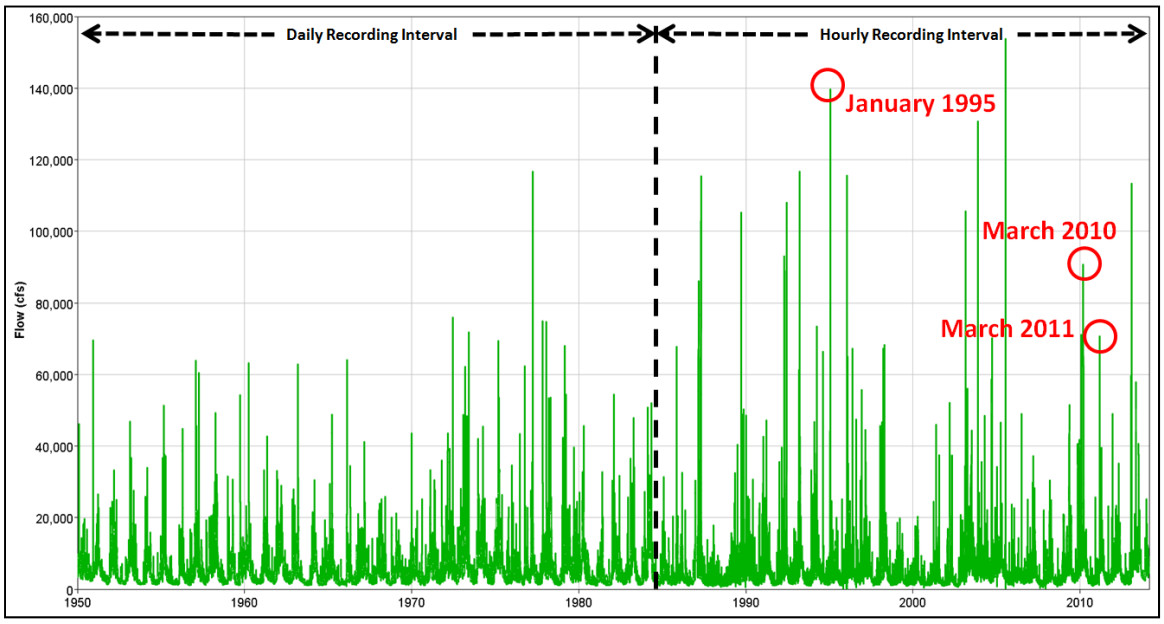

Figure 10. Peak recorded discharge at Bluestone Dam (Red circles indicate calibration events considered for this IDF study.)

3.1.1.5 Results from Calibration Events

The hydrologic model was calibrated for three (3) storm events (January 1995, March 2010, and March 2011) to develop runoff parameters capable of accurately predicting runoff throughout the watershed. A thorough understanding of the development of the hydrologic model, coupled with familiarity with the watershed can allow for the calibration results to be finely tuned in order to obtain a minimal amount of error in recreating historic events. However, since the main objective for the development of this model is to predict runoff from a storm event several magnitudes larger than any that has been recorded previously, consideration must be given to the modeling technique and any associated constraints.

The Snyder Synthetic Unit Hydrograph parameters for the gaged sub-basins were used to calculate the runoff characteristics for the ungaged sub-basins within the watershed based on a process referred to as a Snyder Transfer. The Snyder Transfer process relates the basin characteristics (e.g. longest flow path and centroid longest flow path) to the time to peak and unit peak discharge of gaged basins to ungaged basins. This process has been widely used for the estimation of response from ungaged basins and can be referenced in most hydrology texts. No modifications to the calculated runoff parameters for the ungaged basins were made in order to preserve the integrity of the process.

During the calibration process, observed inflows from upstream watersheds were used as input into the model. This calibration strategy allows for error within the model to be isolated and prevents the downstream calibration events from being influenced from upstream discrepancies between modeled and observed flow events.

Results of the calibration event proved acceptable and are summarized in Table 6 through Table 8. The storm events used for calibration were chosen based on events at particular gages of interest and that also produced a large inflow at Bluestone Dam. Due to the size of the watershed above Bluestone Dam and the spatial distribution/timing of the precipitation, all sub-basins did not have large discharges for all events. Given this consideration, the calibration results of some sub-basins that were parameterized for large storm events, but did not receive a significant volume of precipitation for other calibration events, reproduce the observed data with some error; but within reasonable bounds.

Table 6. Comparison of computed and measured peak flow and volume for the January 1995 calibration event

Gage Location	Peak Flow Calculated (cfs)	Peak Flow Observed (cfs)	Peak Flow Difference	Volume Calculated (in)	Volume Observed (in)
Galax, VA	68,700	68,100	1%	2.41	3.28
Allisonia, VA	110,100	107,100	3%	2.10	2.44
Graysontown, VA	8,000	8,100	-1%	1.13	1.13
Radford, VA	119,200	107,500	10%	1.85	2.06
Bane, VA	5,800	5,700	2%	1.20	1.19
Narrows, VA	9,100	9,100	0%	2.02	2.15
Glen Lyn, VA	131,700	123,500	-6%	1.57	1.81
Falls Mills, VA	1,300	1,300	0%	1.48	2.06
Pipestem, WV	7,900	8,000	-1%	1.11	1.28
Bluestone Dam	145,300	139,800	4%	1.44	1.55

Table 7. Comparison of computed and measured peak flow and volume for the March 2010 calibration event

Gage Location	Peak Flow Calculated (cfs)	Peak Flow Observed (cfs)	Peak Flow Difference	Volume Calculated (in.)	Volume Observed (in.)
Jefferson, NC	2,700	2,700	0%	0.96	0.93
Galax, VA	15,200	15,200	0%	1.01	1.08
Allisonia, VA	32,100	31,900	1%	0.96	1.16
Graysontown, VA	4,000	4,000	0%	0.58	0.64
Radford, VA	40,900	37,900	7%	0.95	1.04
Bane, VA	20,800	20,500	1%	2.47	2.67
Narrows, VA	15,400	15,200	1%	2.88	3.20
Glen Lyn, VA	62,000	71,000	-13%	1.23	1.33
Falls Mills, VA	1,600	1,600	0%	1.79	2.08
Pipestem, WV	23,500	23,400	1%	2.50	2.86
Bluestone Dam	94,500	90,800	4%	1.38	1.57

Table 8. Comparison of computed and measured peak flow and volume for the March 2011 calibration event

Gage Location	Peak Flow Calculated (cfs)	Peak Flow Observed (cfs)	Peak Flow Difference	Volume Calculated (in.)	Volume Observed (in.)
Jefferson, NC	4,100	4,100	0%	0.70	0.93
Galax, VA	20,300	20,300	0%	0.78	0.88
Allisonia, VA	40,300	41,000	1%	0.80	0.86
Graysontown, VA	5,200	5,300	1%	0.45	0.51
Radford, VA	50,100	50,400	1%	0.76	0.77
Bane, VA	11,200	11,200	0%	1.22	1.32
Narrows, VA	6,400	6,400	0%	1.15	1.19
Glen Lyn, VA	62,400	65,100	-4%	0.82	0.82
Pipestem, WV	3,600	3,400	6%	0.50	0.56
Bluestone Dam	66,900	70,700	-5%	0.77	0.73

3.1.2 GIS Terrain Data and Layers

Several types GIS data layers were used to perform the hydrologic analysis of the study area. The data, source, and description are summarized in Table 9. Detailed discussion of their use is provided in subsequent sections of this report.

Table 9. Summary of geospatial data

Data	Description and Source
DEM	10m DEM data was used for the hydrologic analysis for this study. Source: http://nationalmap.gov/viewer.html
National Hydrography Dataset	Contains published stream, reservoirs, and subbasin boundaries. This information was used to verify/edit the DEM data to ensure the correct drainage and subbasin network was delineated. Source: http://nhd.usgs.gov/

3.1.3 Streamflow Data

Hourly stream flow data was obtained from both the USACE - Huntington District and the USGS. Table 10 lists the stream flow gages used to calibrate the rainfall-runoff model and Figure 11 shows their location within the watershed.

Table 10. Stream flow gages used to calibrate the rainfall-runoff model

Gage	Station ID	Drainage Area (sq. mi.)	Latitude	Longitude
South Fork New River near Jefferson, NC	03161000	206	36.39330	-81.40690
New River near Galax, VA	03164000	1141	36.64740	-80.97900
New River at Allisonia, VA	03168000	2211	36.93760	-80.74560
Little River at Graysontown, VA	03164002	309	37.03760	-80.55670
New River at Radford, VA	03171000	2951	37.14180	-80.56920
Walker Creek at Bane, VA	03173000	299	37.26820	-80.70950
Wolf Creek near Narrows, VA	03175500	223	37.30570	-80.84980
New River at Glen Lyn, VA	03176500	3966	37.37290	-80.86060
Bluestone River near Pipestem, WV	03179000	395	37.54400	-81.01040

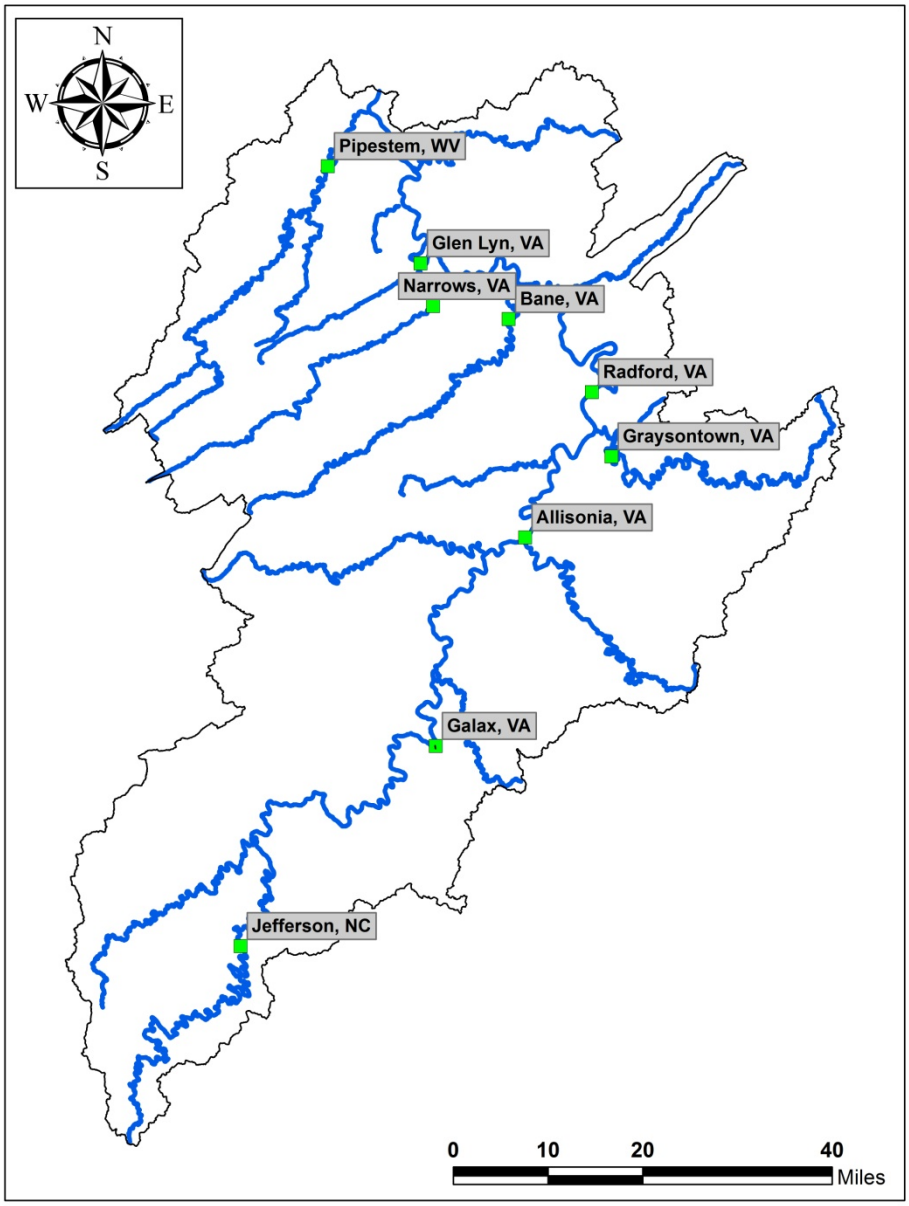

Figure 11. Location of stream flow gages used for the Bluestone Dam rainfall-runoff model

3.2 Methods

3.2.1 Downstream Hydraulic Geometry

Hydraulic geometry refers to the cross-sectional characteristics of a stream which influences the stage-discharge relationship. Deformable alluvial channels are known to adjust their slope, width, depth, and velocity to achieve stable conditions at a specified supply of water and sediment. Downstream hydraulic geometry relationships describe the shape of bank-full alluvial channels in terms of bank-full width, average flow depth, average flow velocity, and channel slope (Julien, 1995). The downstream hydraulic geometry relationships are derived from the nonlinear

regression analysis of a large data set (1,485 measurements), consisting of sand, gravel, and cobble bed streams with planform geometry ranging from meandering to braided (Lee, 2006).

3.2.1.1 Governing Equations

The downstream hydraulic geometry of noncohesive alluvial channels can be determined from the stability analysis of sediment particles under 2-dimensional flow conditions (Julien, 1995). Four relationships, dominant discharge, resistance to flow, particle stability, and secondary flow, were used to analytically determine the downstream hydraulic geometry relationships.

3.2.1.1.1. Dominant Discharge

The dominant discharge has the magnitude and frequency that defines the dimensions of an alluvial channel. In defining the downstream hydraulic geometry, the dominant discharge is set equal to the bankfull discharge, the discharge corresponding to a return period of approximately 1.5 years.

The dominant discharge, as shown in Figure 12, is determined assuming steady-uniform bankfull flow conditions as:

$$Q = WhV$$

where

W = top width (m)

h = flow depth (m)

V = average flow velocity (m/s)

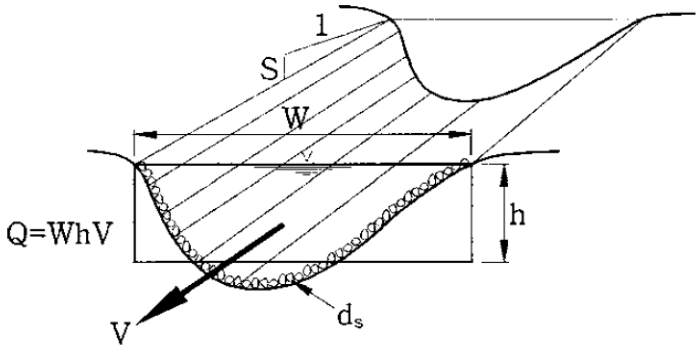

Figure 12. Cross-section Schematic

3.2.1.1.2. Resistance to Flow

The flow resistance of an alluvial channel is expressed in power form as:

$$V = a\sqrt{g}\left(\frac{h}{d_s}\right)^m h^{1/2} S^{1/2}$$

where

g = gravitational acceleration (m/s^2)

h = flow depth (m)

d_s = median grain size, d_{50} (m)

S = slope (m/m)

m = resistance exponent = $\frac{1}{\ln^{12.2h}/_{d_s}}$

3.2.1.1.3. Particle Stability

Particle stability in non-cohesive straight alluvial channels is determined as the ratio of two forces, relative magnitude of the downstream shear force and the particle weight. This ratio is defined as the Shields number and is expressed as:

$$\tau_* = \frac{hS}{(G-1)d_s}$$

where

h = flow depth (m)

S = slope (m/m)

G = specific gravity of sediment particles

d_s = median grain size, d_{50} (m)

Incipient motion of non-cohesive particles in turbulent flows over rough boundaries is the critical value of the Shields number, $\tau_* \approx 0.047$.

3.2.1.1.4. Secondary Flows

The downstream orientation of curved channels changes, secondary circulation occurs where streamlines near the surface are directed towards the outer bank and the streamlines near the bed are directed towards the inner bank. This is quantified as:

$$tan\,\lambda = b_r \left(\frac{h}{d_s}\right)^{2m} \frac{h}{W}$$

where

λ = streamline deviation angle

b_r = constant

h = flow depth (m)

d_s = median grain size, d_{50} (m)

m = resistance exponent = $\frac{1}{\ln^{12.2h}/_{d_s}}$

W = top width (m)

3.2.1.2 J-W Equations

The downstream hydraulic geometry of non-cohesive alluvial channels with hydraulically turbulent flows were derived for flow depth, top width, average flow velocity, and slope as:

$$h = 0.133\, Q^{\frac{1}{3m+2}}\, d_s^{\frac{6m-1}{6m+4}}\, \tau_*^{\frac{-1}{6m+4}}$$

$$W = 0.512\, Q^{\frac{2m+1}{3m+2}}\, d_s^{\frac{-4m-1}{6m+4}}\, \tau_*^{\frac{-2m-1}{6m+4}}$$

$$V = 14.7\, Q^{\frac{m}{3m+2}}\, d_s^{\frac{2-2m}{6m+4}}\, \tau_*^{\frac{2m+2}{6m+4}}$$

$$S = 12.4\, Q^{\frac{-1}{3m+2}}\, d_s^{\frac{5}{6m+4}}\, \tau_*^{\frac{6m+5}{6m+4}}$$

where

h = flow depth (m)

W = top width (m)

V = average flow velocity (m/s)

S = slope (m/m)

Q = dominant discharge (m^3/s)

d_s = median grain size, d_{50} (m)

τ_* = Shields Parameter

m = resistance exponent = $\frac{1}{\ln^{12.2h}/_{d_{50}}}$

The equations can be simplified when Manning's equation is applicable and m = 1/6 to:

$$h \cong 0.133 Q^{0.4} \tau_*^{-0.2}$$

$$W \cong 0.512 Q^{0.53} d_s^{-0.33} \tau_*^{-0.27}$$

$$V \cong 14.7 Q^{0.07} d_s^{0.33} \tau_*^{0.47}$$

$$S \cong 12.4 Q^{-0.4} d_s\, \tau_*^{1.2}$$

Julien and Wargadalam (1995) empirically recalibrated the equations to:

$$h = 0.2\, Q^{\frac{2}{5+6m}}\, d_s^{\frac{6m}{5+6m}}\, S^{\frac{-1}{5+6m}}$$

$$W = 1.33\, Q^{\frac{2+4m}{5+6m}}\, d_s^{\frac{-4m}{5+6m}}\, S^{\frac{-1-2m}{5+6m}}$$

$$V = 3.76\, Q^{\frac{1+2m}{5+6m}}\, d_s^{\frac{-2m}{5+6m}}\, S^{\frac{2+2m}{5+6m}}$$

$$\tau_* = 0.121\, Q^{\frac{2}{5+6m}}\, d_s^{\frac{-5}{5+6m}}\, S^{\frac{4+6m}{5+6m}}$$

The equations can be simplified when Manning's equation is applicable (m = 1/6) to:

$$h \cong 0.2 Q^{0.33} d_s^{0.17} S^{-0.17}$$

$$W \cong 1.33 Q^{0.44} d_s^{-0.11} S^{-0.22}$$

$$V \cong 3.76 Q^{0.22} d_s^{-0.05} S^{0.39}$$

$$\tau_* \cong 0.121 Q^{0.33} d_s^{-0.83} S^{0.83}$$

The effects of sediment discharge Q_{bv} on the downstream hydraulic geometry is determined by substituting a function of the bed-material discharge for slope, S, resulting in the following equations:

$$h \cong 0.19 Q^{0.46} d_s^{0.13} Q_{bv}^{-0.12}$$

$$W \cong 1.3 Q^{0.62} d_s^{-0.15} Q_{bv}^{-0.15}$$

$$V \cong 4 Q^{-0.08} d_s^{0.02} Q_{bv}^{0.27}$$

$$S \cong 1.2 Q^{-0.77} d_s^{0.19} Q_{bv}^{0.69}$$

$$\tau_* \cong 0.14 Q^{-0.31} d_s^{-0.67} Q_{bv}^{0.57}$$

The impact of the bed-material sediment concentration $C_{mg/l}$ at the dominant discharge can be determined by substituting $Q_{bv} = 3.8 \times 10^{-7}\, C_{mg/l}\, Q$, resulting in the following equations:

$$h \cong 1.1 Q^{0.34} d_s^{0.13} C_{mg/l}^{-0.12}$$

$$W \cong 12 Q^{0.47} d_s^{-0.15} C_{mg/l}^{-0.15}$$

$$V \cong 0.075 Q^{0.19} d_s^{0.02} C_{mg/l}^{0.27}$$

$$S \cong 4.4x10^{-5} Q^{-0.08} d_s^{0.19} C_{mg/l}^{0.69}$$

$$\tau_* \cong 3x10^{-5} Q^{0.26} d_s^{-0.67} C_{mg/l}^{0.57}$$

3.2.2 Muskingum-Cunge Model

Channelized runoff continuously transforms while travelling in the downstream direction as indicated by inspection of flood hydrographs. The hydrograph characteristics change based on the flow hydraulics, storage within the channel, subsurface gains and losses, and lateral inflow into the channel. In order to accurately model a large watershed or drainage network, a hydrologic routing method is preferred due to the improved computational speed and reduced amount of detailed field data required, as compared to traditional 1-dimensional hydraulic models (Garbrecht, 1991).

Hydrologic routing methods used to model channelized flow from individual subbasins throughout the watershed are based on the St. Venant equations,

neglecting the interia term. The solution is based on the finite difference method formulated from the original partial differential equations. The Muskingum-Cunge model is based on a convective diffusion equation determined through linear approximation of the continuity and momentum equations.

3.2.2.1 Governing Equations

The following form of the continuity equation was used:

$$\frac{\partial A}{\partial t} + \frac{\partial Q}{\partial x} = q_l$$

where

A = flow area (ft^2)

t = time (s)

Q = flow rate (cfs)

x = reach length (ft)

q_l = lateral flow (cfs/ft)

The diffuse form of the momentum equation was used:

$$S_f = S_o - \frac{\partial y}{\partial x}$$

where

S_f = friction slope

S_o = bed slope

y = flow depth (ft)

x = reach length (ft)

Combination of the continuity and momentum equations using linear approximations results in the convective diffusion equation:

$$\frac{\partial Q}{\partial t} + c\frac{\partial Q}{\partial x} = \mu\frac{\partial^2 Q}{\partial x^2} + cq_l$$

where

Q = flow rate (cfs)

t = time (s)

x = reach length (ft)

q_l = lateral flow (cfs/ft)

c = wave celerity = $\frac{dQ}{dA}$ (ft)

μ = hydraulic diffusivity = $\frac{Q}{2BS_o}\left(\frac{\text{ft}^2}{\text{s}}\right)$

A finite difference approximation of the partial derivatives is then combined with the following equation based on storage within the reach:

$$O_t = \left[\frac{\Delta t - 2KX}{2K(1-X)+\Delta t}\right] I_t + \left[\frac{\Delta t + 2KX}{2K(1-X)+\Delta t}\right] I_{t-1} + \left[\frac{2K(1-X)-\Delta t}{2K(1-X)+\Delta t}\right] O_{t-1}$$

where

O_t= outflow hydrograph ordinate at time t

I_t= inflow hydrograph ordinate at time t

t = time (s)

K = storage coefficient

X = dimensionless weighting factor $(0 \leq X \leq 0.5)$

Combination of these equations results in the following approximation:

$$O_t = C_1 I_{t-1} + C_2 I_t + C_3 O_{t-1} + C_4 (q_l \Delta x)$$

$$C_1 = \frac{\frac{\Delta t}{K} + 2X}{\frac{\Delta t}{K} + 2(1-X)}$$

$$C_2 = \frac{\frac{\Delta t}{K} - 2X}{\frac{\Delta t}{K} + 2(1-X)}$$

$$C_3 = \frac{2(1-X) - \frac{\Delta t}{K}}{\frac{\Delta t}{K} + 2(1-X)}$$

$$C_4 = \frac{2\left(\frac{\Delta t}{K}\right)}{\frac{\Delta t}{K} + 2(1-X)}$$

The value of the storage coefficient (K) and weighting factor (X) are determined from physically based parameters and are equal to:

$$\text{K} = \frac{\Delta x}{c}$$

$$\text{X} = \frac{1}{2}\left(1 - \frac{Q}{BS_o c \Delta x}\right)$$

where

Δx = space increment of finite difference cell

$c = \text{wave celerity} = \frac{dQ}{dA}$ (ft)

$q = \text{unit width discharge } \left(\frac{\text{cfs}}{\text{ft}}\right) = \frac{Q}{B}$

Q = flow rate (cfs)

B = top width (cfs)

S_o = channel bed slope

3.2.2.2 8-Point Cross Section

The Muskingum-Cunge model is able to account for floodplain storage and varying conveyance between the main channel and overbank areas. This is important when analyzing large floods, especially floods of the magnitude associated with the Probable Maximum Flood. The Muskingum-Cunge method utilizes an 8-point cross-section to represent the hydraulic geometry of a river reach, as shown in Figure 13.

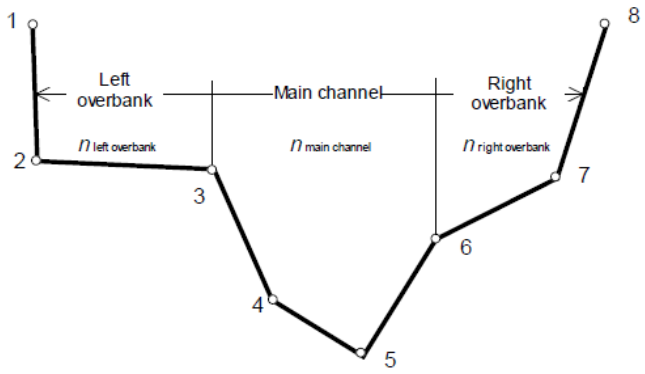

Figure 13. Representative 8-point Cross-Section (from HEC-HMS Technical Reference Manual, 2000)

The physical data of the cross-section is used to calculate the hydraulic properties at intervals ranging from the thalweg to the top of the cross-section. Power functions for discharge, flow area, top width, and flow depth are calculated for the given cross-section using the Manning's uniform flow equation (Garbrecht, 1991). This information is then used inform the storage coefficient (K) and weighting factor (X) variables for use within the Muskingum-Cunge model.

Chapter 4
Analysis

This analysis is focused on the hydrologic routing of channelized flow through a watershed during a large storm event (Probable Maximum Flood). More specifically, the analysis is intended to quantify potential impacts to the routing of large flood events due to changes in hydraulic geometry as a result of continued change in climatic patterns throughout the world.

- Develop hydraulic geometry relative relationship curves based on J-W equations.
- Estimate dominant discharge based on gaged data
- Use J-W equations to develop 8-point cross-sections
- Modify Muskingum-Cunge parameters based on relative relationships
- Route (Base, 100% increase in Q, 500% increase in Q)

4.1 Downstream Hydraulic Geometry Relationships

The downstream hydraulic geometry of a channel is a function of the dominant discharge (Q, m^3/s) and channel width (W, m), average flow depth (h, m), mean flow velocity measured normal to the flow direction (V, m/s), channel slope (S), and Shields number (τ_*). The downstream hydraulic geometry were analyzed by assuming all variables constant, except the dominant discharge which was systematically increased. This analysis focus on the relationship between dominant discharge and width, flow depth, and velocity. The width and flow depth relationships were then used to inform the subsequent modifications to the channel cross-sections for use in the Muskingum-Cunge routing method.

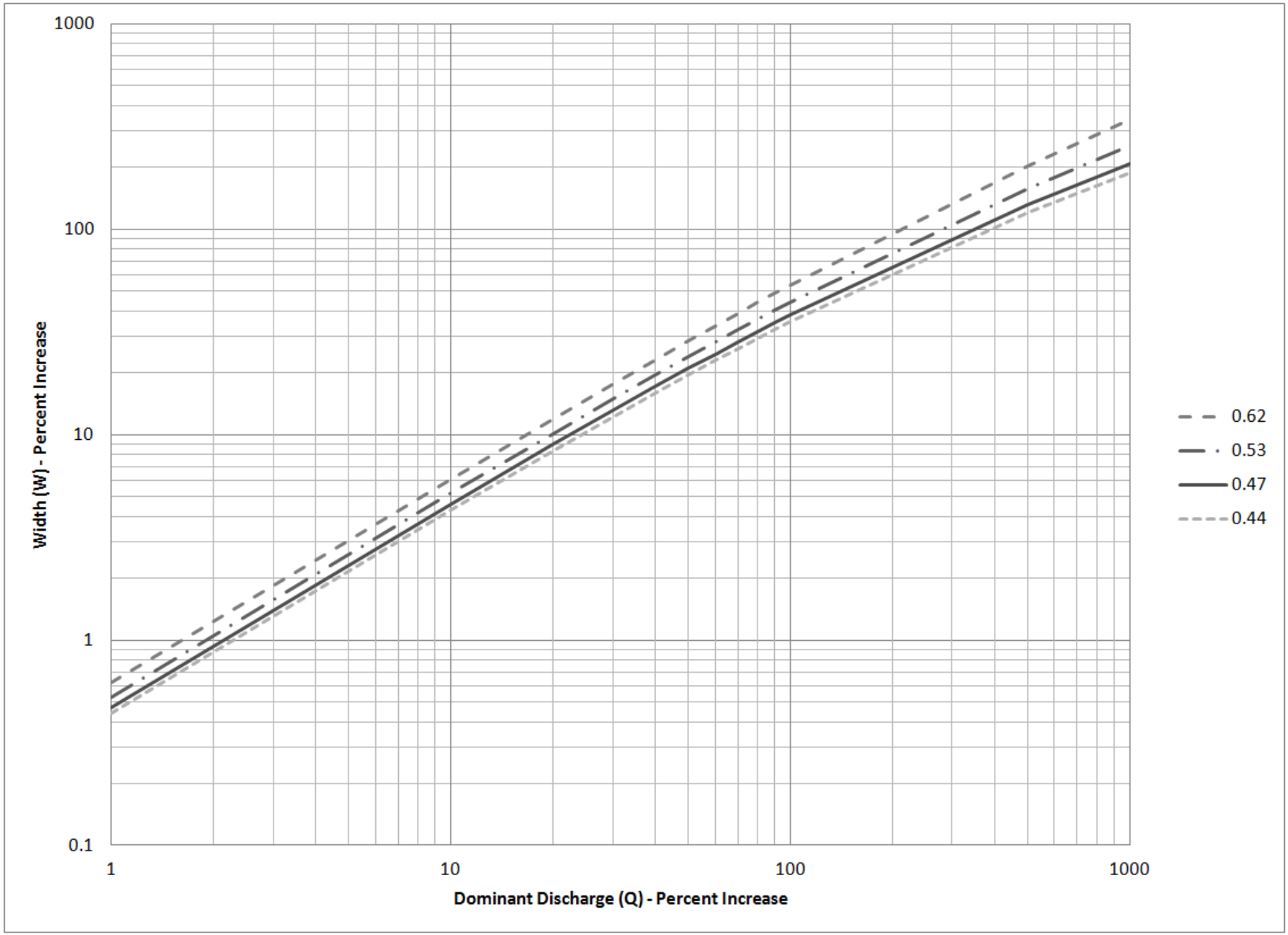

Figure 14. Downstream Hydraulic Geometry Dominant Discharge Relationship – Channel Width

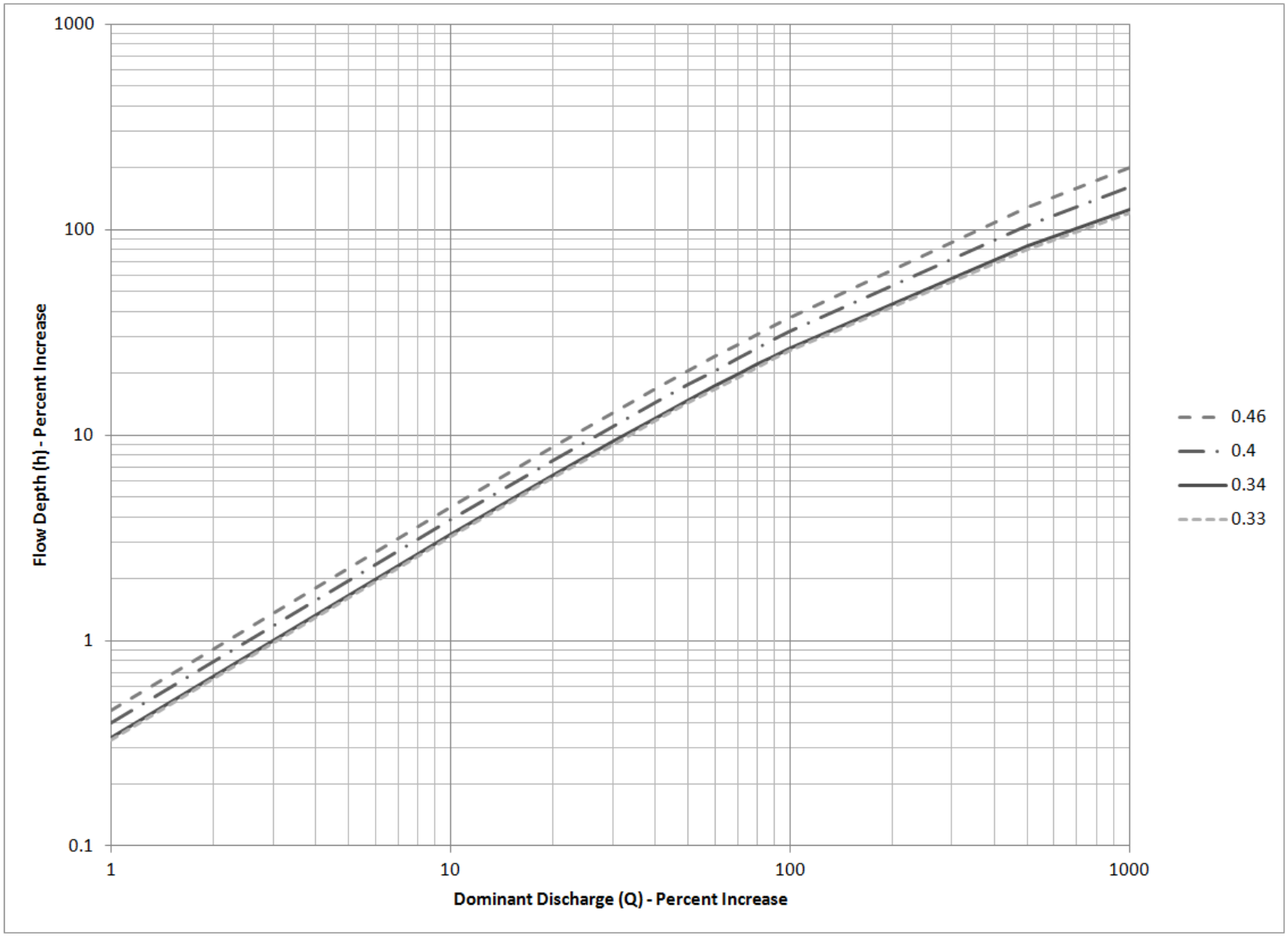

Figure 15. Downstream Hydraulic Geometry Dominant Discharge Relationship – Bankfull Depth

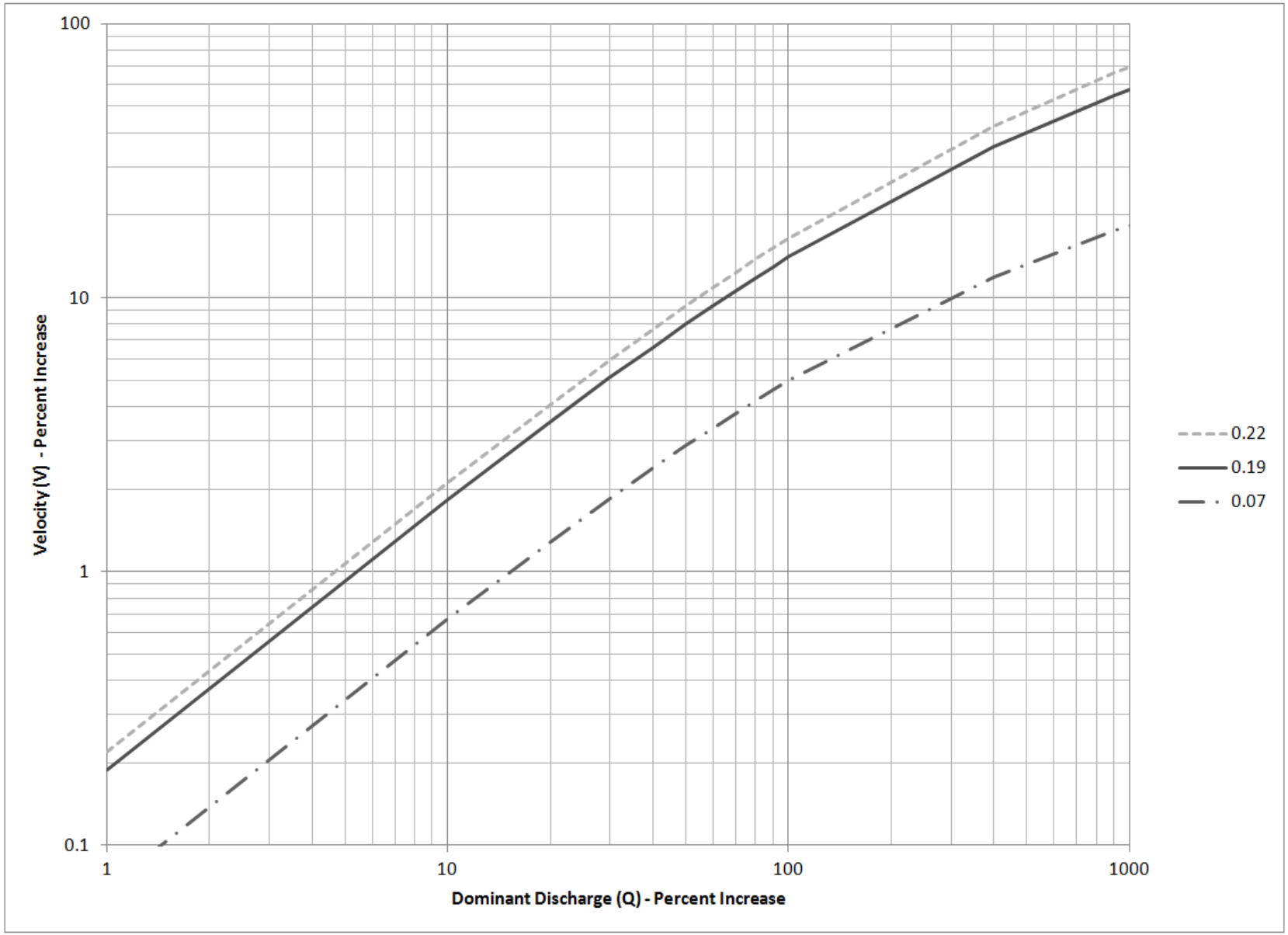

Figure 16. Downstream Hydraulic Geometry Dominant Discharge Relationship - Velocity

4.2 Dominant Discharge

At a given cross-section within a watershed, the range of observed discharges has an associated frequency of occurrence (Leopold, 1953). The forming and maintenance of channel cross-sections and a river's longitudinal profile is a function of the movement of sediment, therefore, the dominant discharge is defined as the discharge capable of transporting the most sediment over a long period of time (Benson, 1966). The dominant discharge along the New River throughout the Bluestone Dam watershed was set to be equal to the 1.5 year storm event. This storm event was determined through the statistical analysis of approximately 30 years of hourly flow data at nine locations throughout the watershed. The dominant discharge for each location is shown in Figure 17 - Figure 25 and summarized in Table 11.

Table 11. Dominant Discharge Summary

Location	1.5 Year Discharge (cms)
Jefferson, NC	70 (1986-2015)
Galax, VA	342 (1984-2015)
Allisonia, VA	579 (1984-2015)
Radford, VA	605 (1986-2015)
Graysontown, VA	64 (1988-2015)
Bane, VA	85 (1986-2015)
Narrows, VA	74 (1988-2015)
Glen Lyn, VA	826 (1984-2015)
Pipestem, WV	127 (1984-2015)

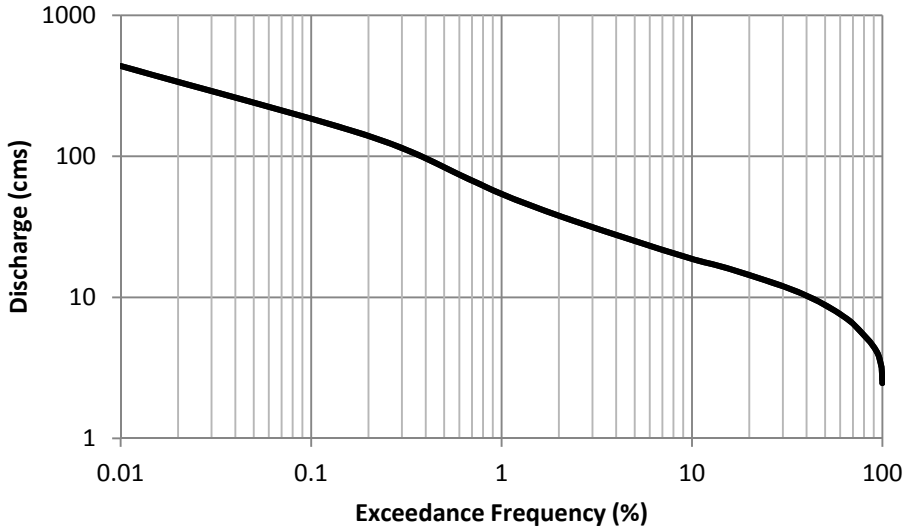

Figure 17. Recurrence Interval Curve for Jefferson, NC

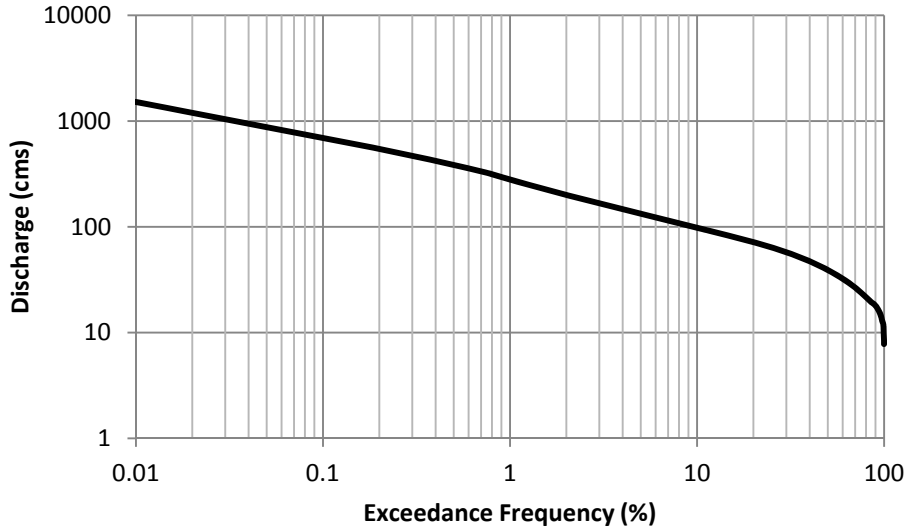

Figure 18. Recurrence Interval Curve for Galax, VA

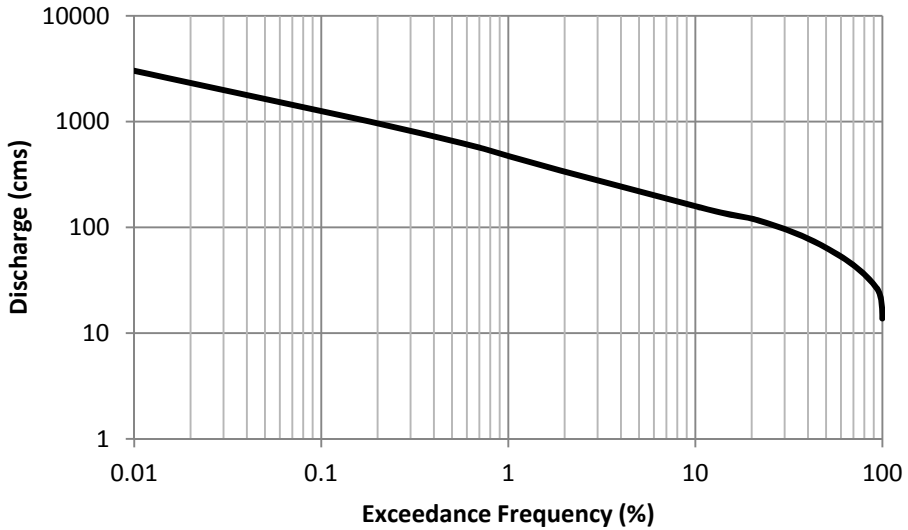

Figure 19. Recurrence Interval Curve for Allisonia, VA

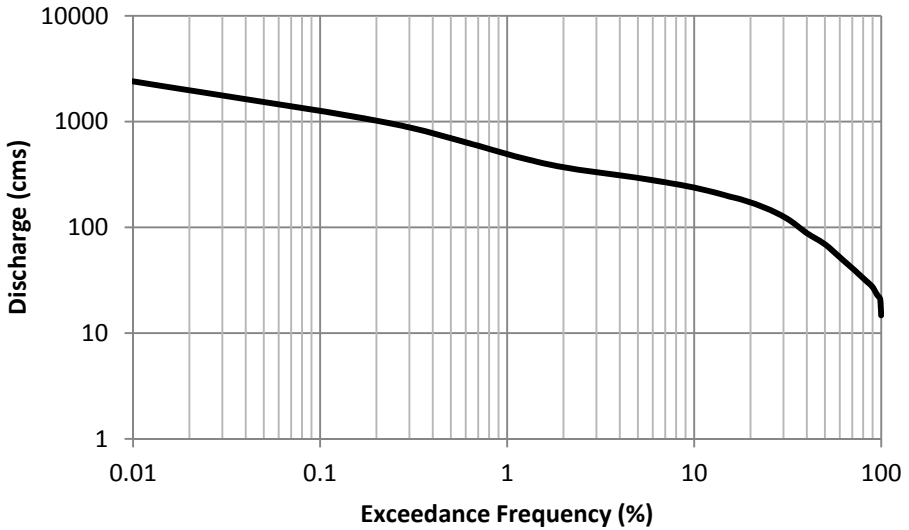

Figure 20. Recurrence Interval Curve for Radford, VA

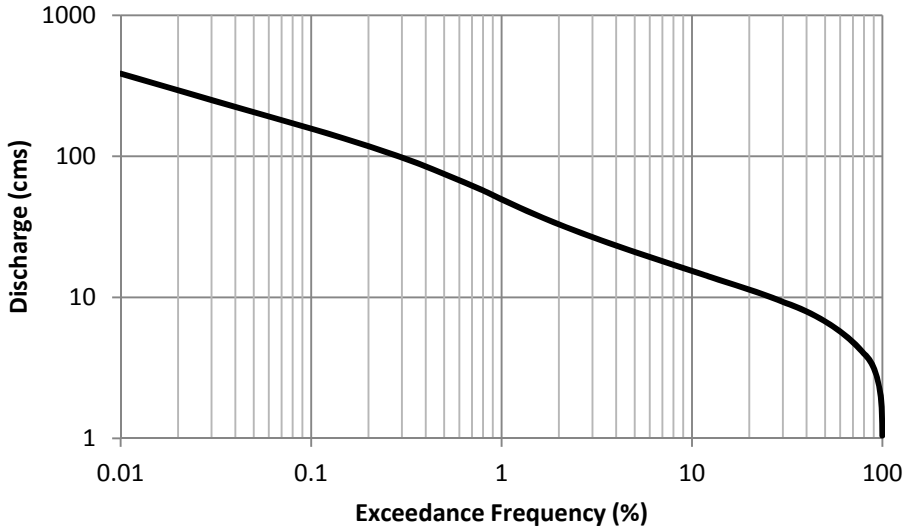

Figure 21. Recurrence Interval Curve for Graysontown, VA

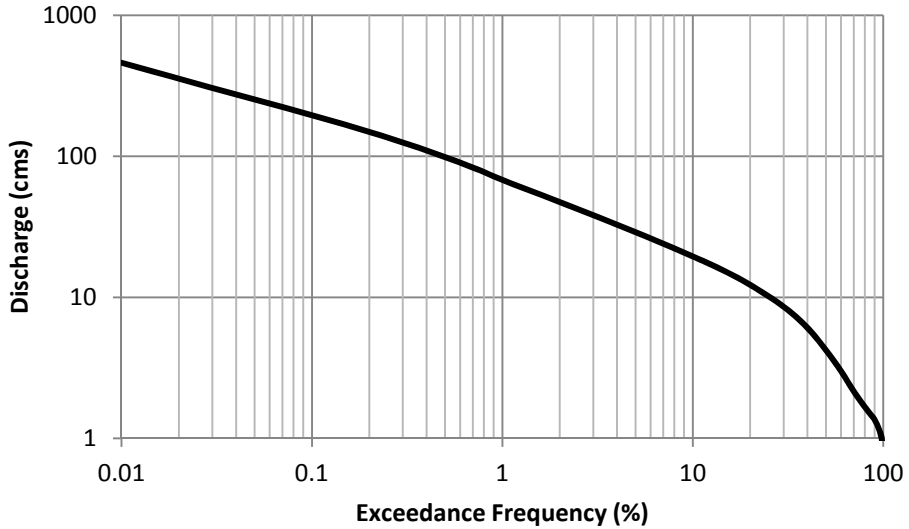

Figure 22. Recurrence Interval Curve for Bane, VA

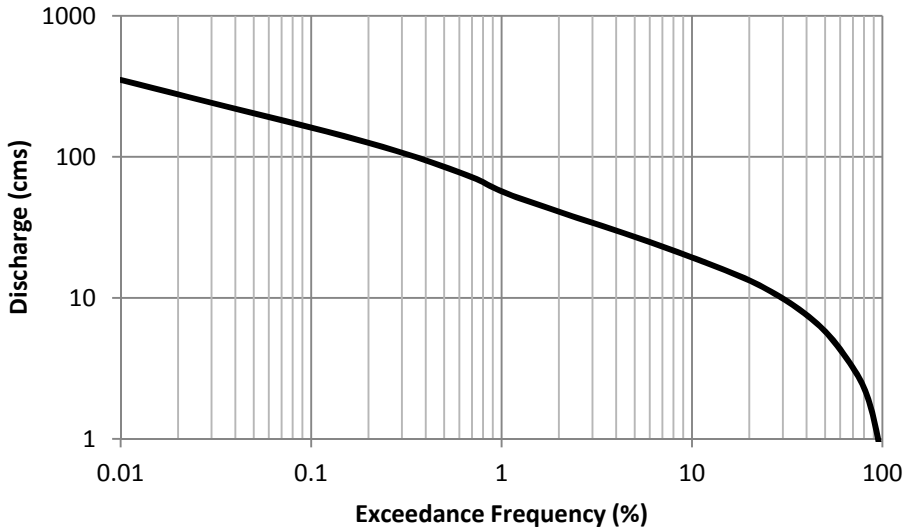

Figure 23. Recurrence Interval Curve for Narrows, VA

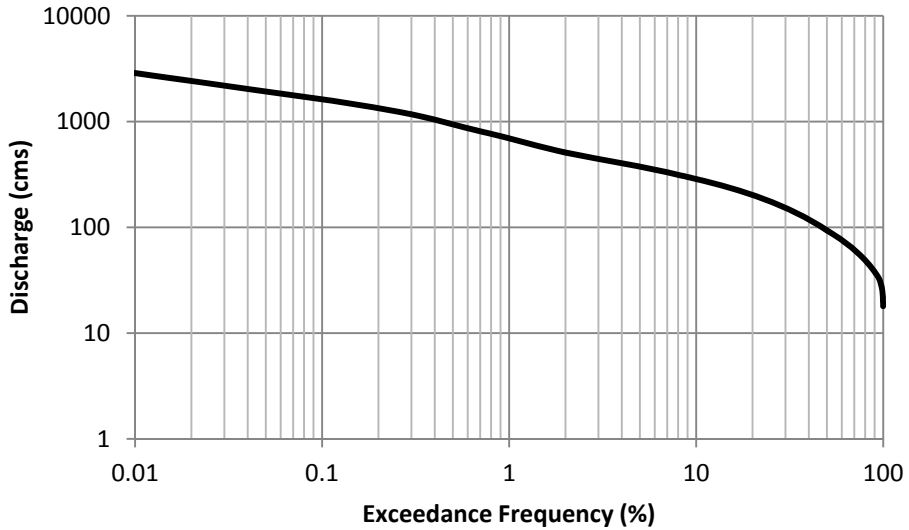

Figure 24. Recurrence Interval Curve for Glen Lynn, VA

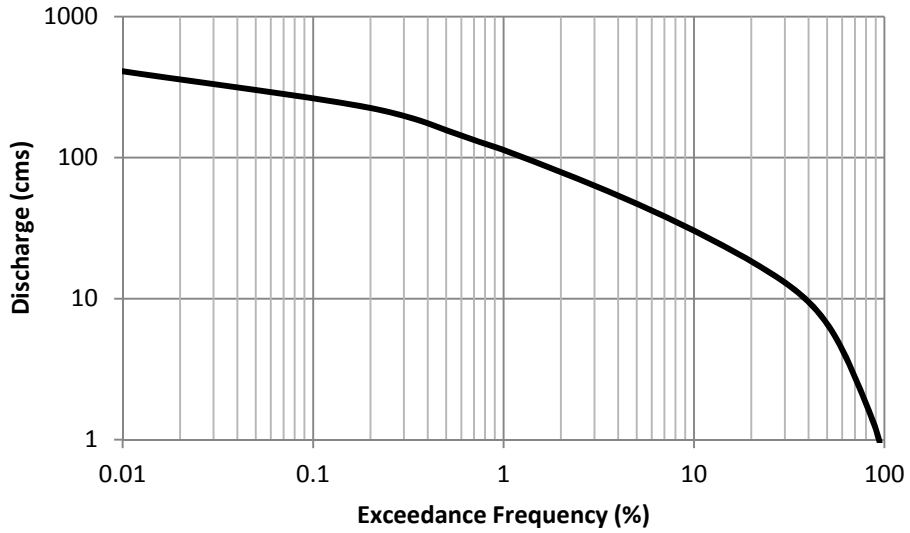

Figure 25. Recurrence Interval Curve for Pipestem, WV

4.3 Cross-Section Data for Muskingum-Cunge Hydrologic Routing

The J-W equations for depth and width were used to set the base conditions for the Muskingum-Cunge 8-point cross-sections. The J-W equations in terms of sediment concentration were used because it was estimated to be the most stable variable for this watershed. The following form of the J-W equations were used for flow depth and top width:

$$h \cong 1.1 Q^{0.34} d_s^{0.13} C_{mg/l}^{-0.12}$$

$$W \cong 12 Q^{0.47} d_s^{-0.15} C_{mg/l}^{-0.15}$$

where

h = flow depth (m)

W = top width (m)

Q = dominant discharge (m^3/s)

d_s = median grain size, d_{50} (m)

$C_{mg/l}$ = sediment concentration (mg/l)

The dominant discharge was determined through the analysis described in Section 4.2 at each gaged location. The median grain size and sediment concentration were assumed to be constant throughout the watershed. The results from the J-W equations were then used to develop the 8-point cross-section for base conditions throughout the watershed. An example cross-section for Allisonia, VA is presented in Figure 26.

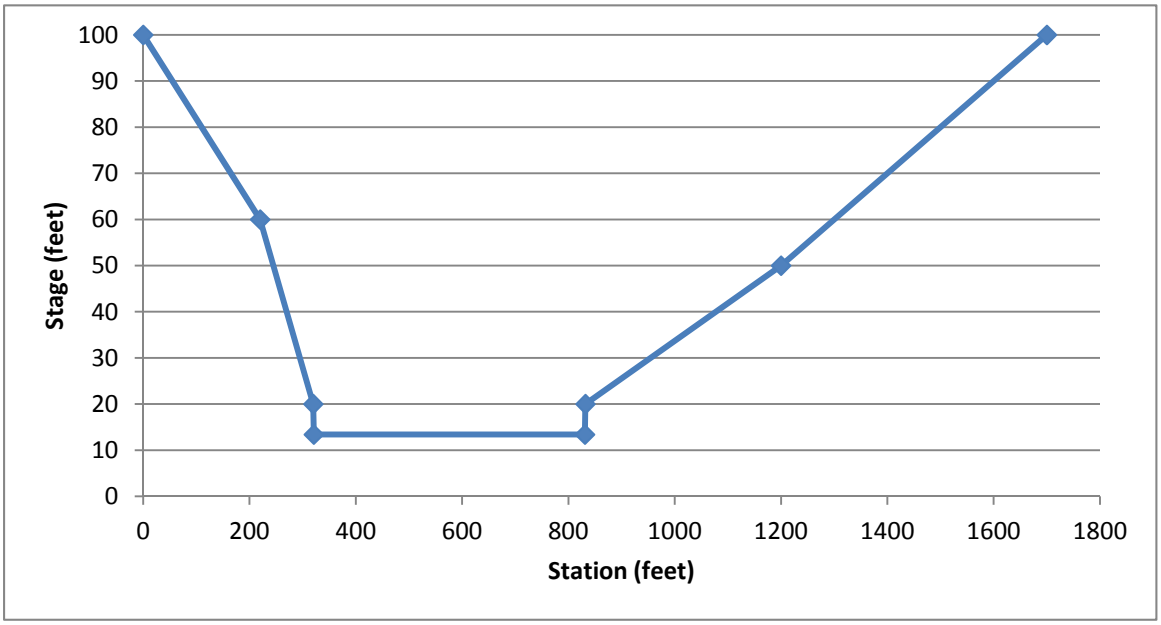

Figure 26. Muskingum-Cunge 8-point Cross-Section at Allisonia, VA

Results of the base condition geometry were then compared to the daily operational model used by USACE, aerial imagery, and topographic mapping of the watershed along the gaged reaches. The gage near Allisonia, VA has an estimated dominant discharge of 656 cms which resulted in a calculated width based on the downstream hydraulic geometry equations equal to 512 feet. This is compared to the measured value from the data sources listed above, and shown in Figure 27, of 550 feet wide, less than a 10-percent difference. Therefore, the downstream hydraulic geometry equations were deemed acceptable for the study area. Verification of the gaged locations along the main stem of the New River are located in Appendix A.

Figure 27. Current conditions near Allisonia, VA

4.4 Cross-Section Data Modification to Account for Climate Change

To analyze the impact of flood routing attenuation through the watershed as a result of increased dominant discharge, the dimensions of the 8-point cross-sections were then modified for two additional scenarios, 100% and 500% increase in dominant discharge. The changes to the hydraulic geometry (width and depth) were then determined given the information from Section 4.1. The percentage increase for both width and flow depth are graphically shown in Figure 28 and Figure 29 and summarized in Table 12.

This information was then used to make adjustments to all of the cross-sections within the watershed. Results of the modifications are summarized in Table 13 and graphically depicted in Figure 30 through Figure 38.

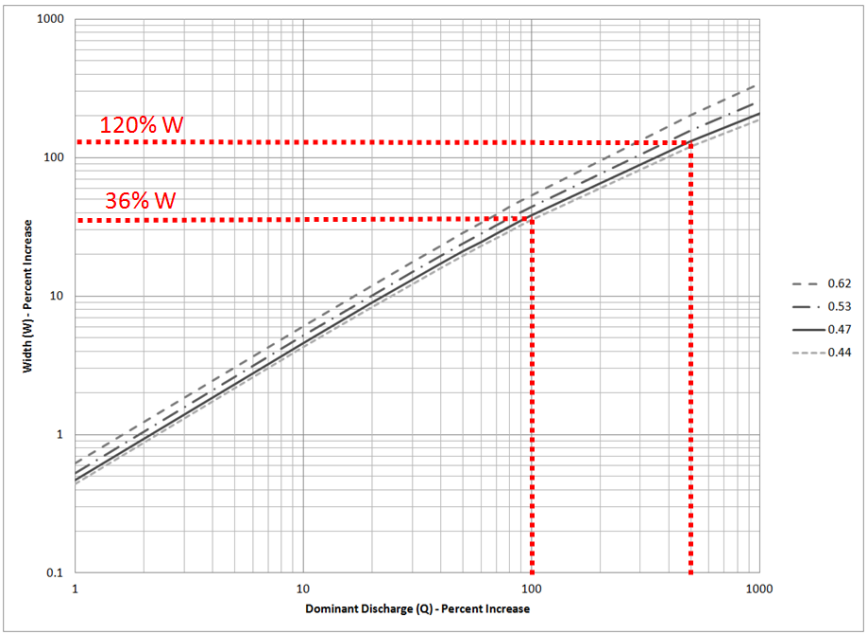

Figure 28. Change in width based on increased dominant discharge.

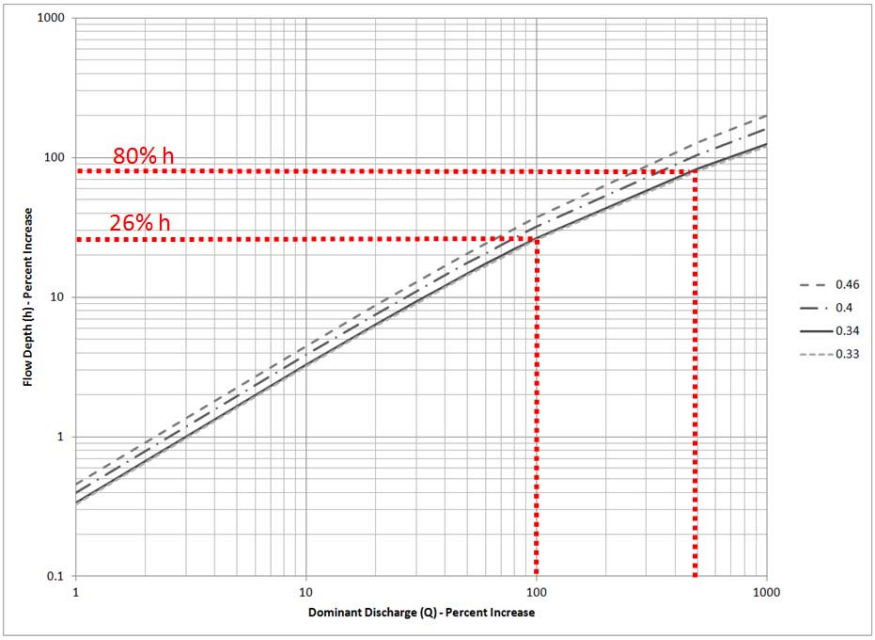

Figure 29. Change in flow depth based on increased dominant discharge.

Table 12. Summary of downstream hydraulic geometry relationships with respect to an increase in dominant discharge.

Scenario	Width Increase (%)	Flow Depth Increase (%)
100% Q	36	26
500% Q	120	80

Table 13. Cross-Section Data Based on J-W Equations

		Jefferson	Galax	Allisonia	Radford	Graysontown	Bane	Narrows	Glen Lynn	Pipestem
Width (ft)	**Base**	162	381	512	548	191	207	171	687	220
	100%	220	517	695	744	259	281	232	932	299
	500%	356	838	1126	1206	420	455	376	1511	484
Depth (ft)	**Base**	3	5.5	6.6	6.7	3.3	3.5	3	7.9	3.3
	100%	3.8	6.9	8.3	8.4	4.1	4.4	3.8	9.9	4.1
	500%	5.4	9.9	11.9	12.1	6.0	6.3	5.4	14.3	6.0

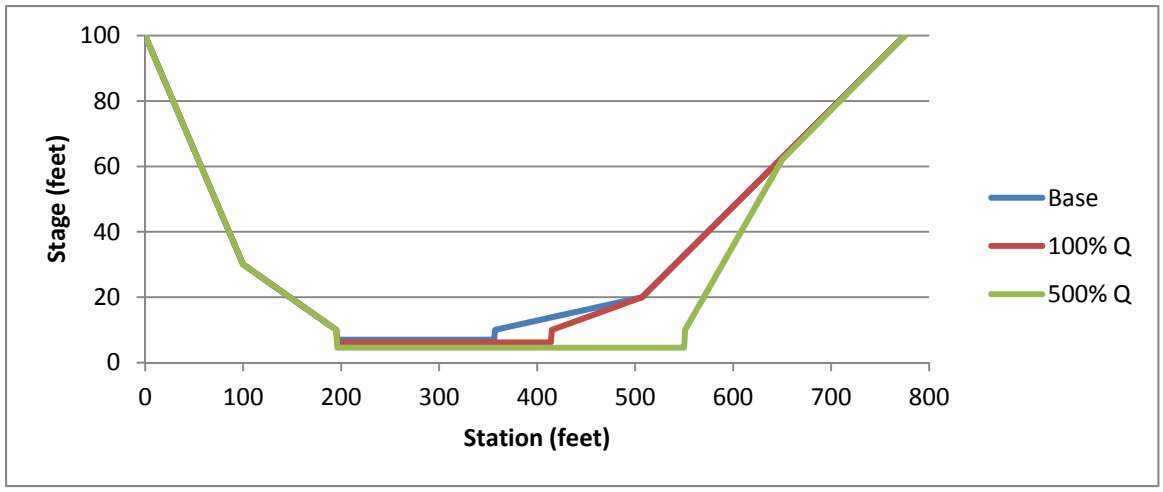

Figure 30. 8-Point Cross-Section at Jefferson, NC

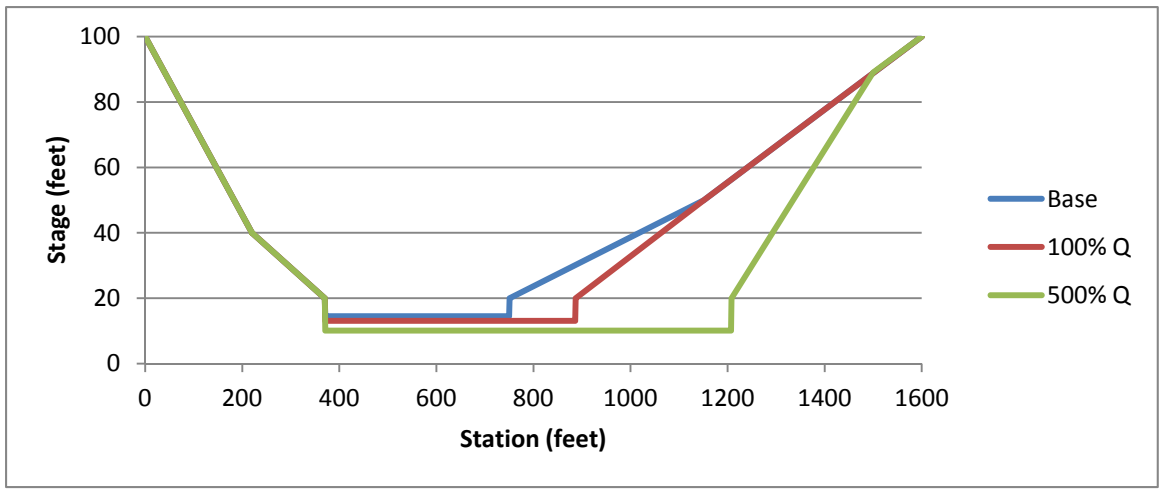

Figure 31. 8-Point Cross-Section at Galax, VA

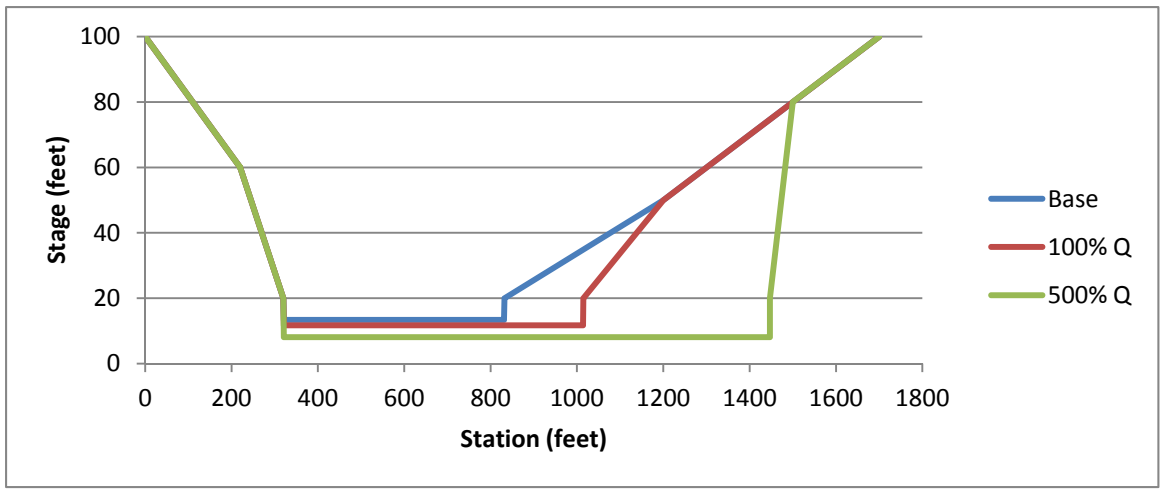

Figure 32. 8-Point Cross-Section at Allisonia, VA

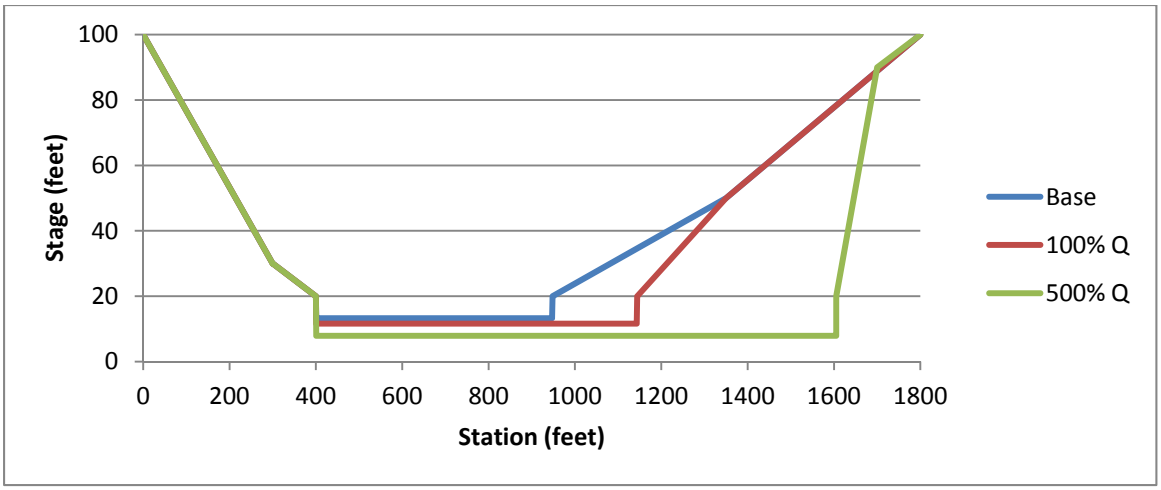

Figure 33. 8-Point Cross-Section at Radford, VA

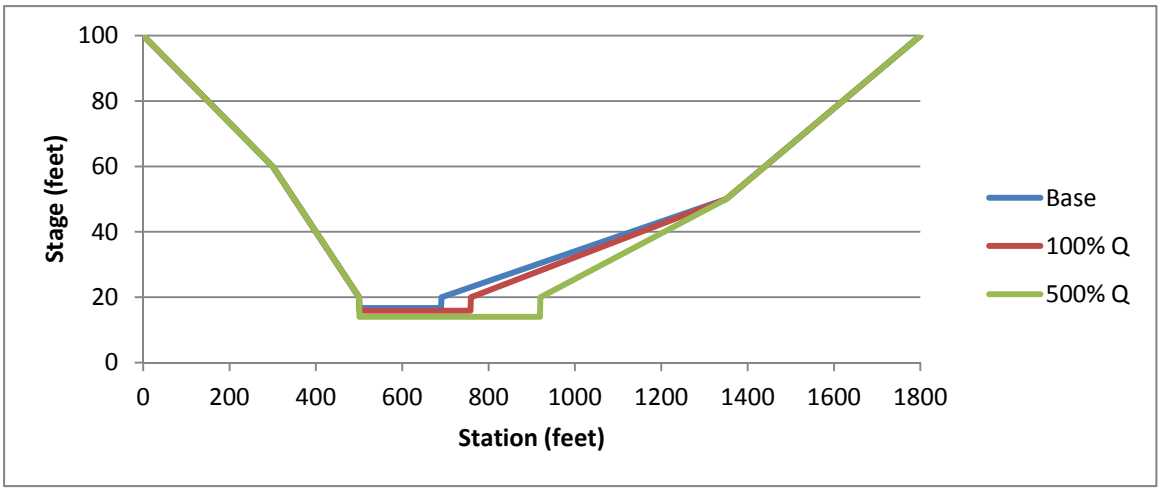

Figure 34. 8-Point Cross-Section at Graysontown, VA

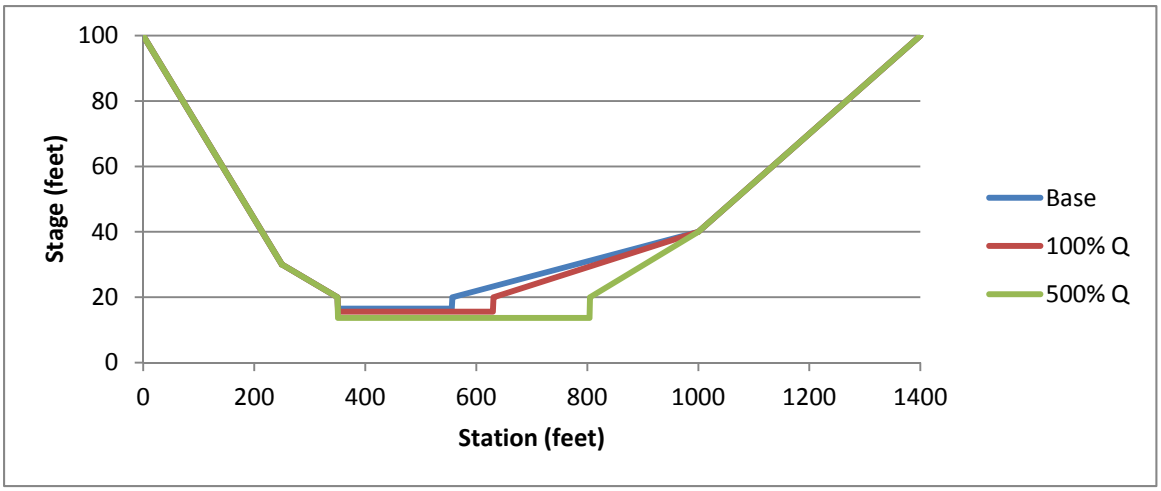

Figure 35. 8-Point Cross-Section at Bane, VA

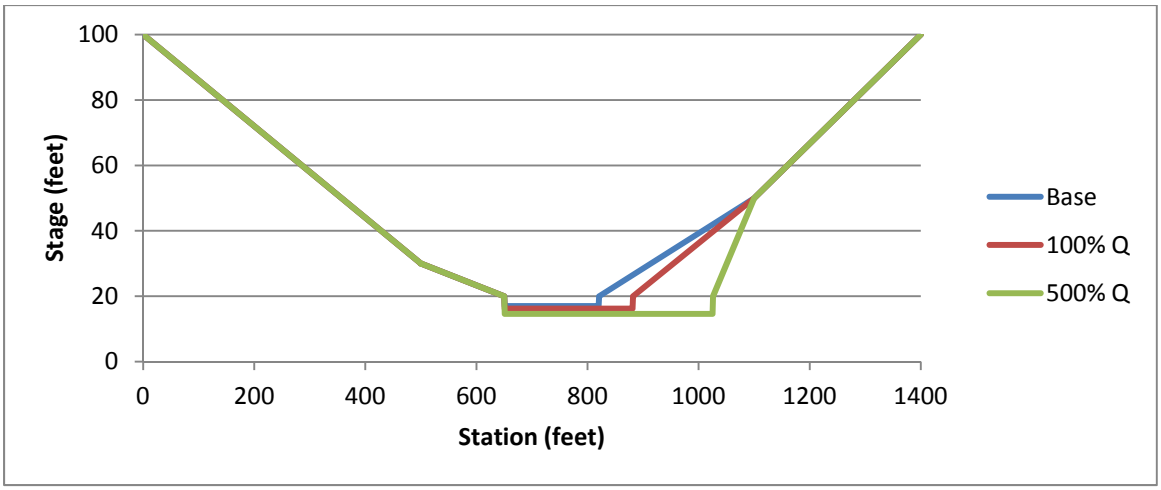

Figure 36. 8-Point Cross-Section at Narrows, VA

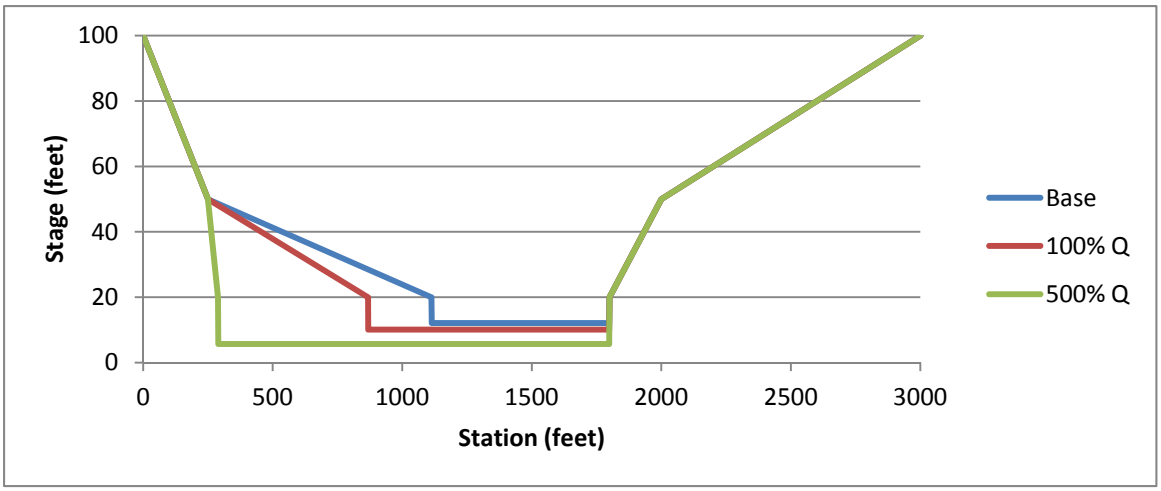

Figure 37. 8-Point Cross-Section at Glen Lynn, VA

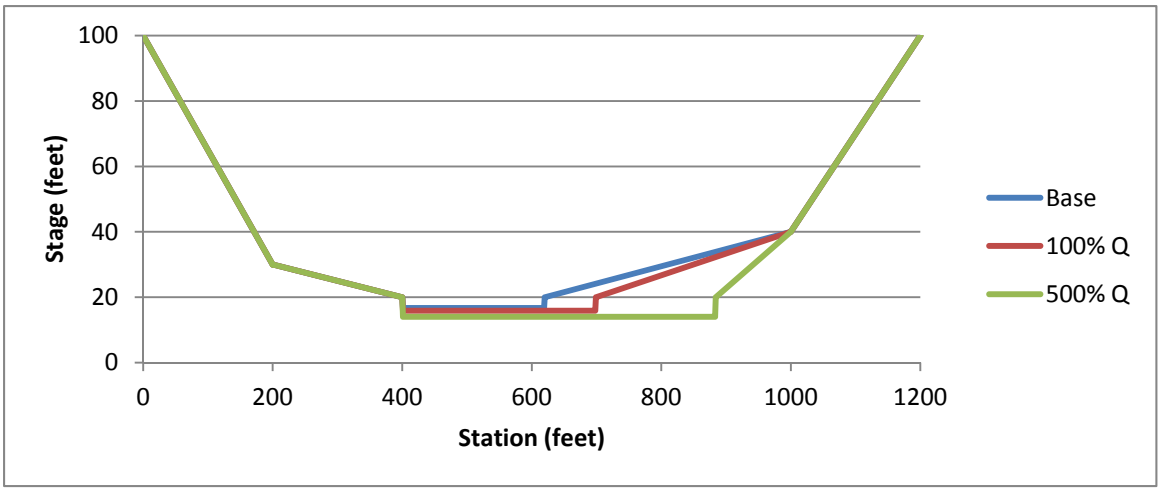

Figure 38. 8-Point Cross-Section at Pipestem, VA

4.5 Hydrologic Routing Results

The hydrologic routing parameters for the Bluestone watershed were systematically altered according the analyses presented in the previous sections. The Bluestone Dam Inflow Design Flood (IDF) was routed through the watershed for each scenario with the only change being to the Muskingum-Cunge 8-point cross-section data. This allowed for a comparison of the peak discharge and timing of the flood hydrograph at Bluestone Dam as it is impacted from changes of the downstream hydraulic geometry. Results of this application to the Bluestone Dam watershed are summarized for all scenarios in Table 14 and presented graphically in Figure 39.

Table 14. Summary of Hydrologic Routing

Scenario	Time to Peak Discharge (hours)	Peak Discharge (cfs)
Base	53	1,387,100
100% Q	52	1,430,300 (3.1% increase)
500% Q	51	1,475,900 (6.4% increase)

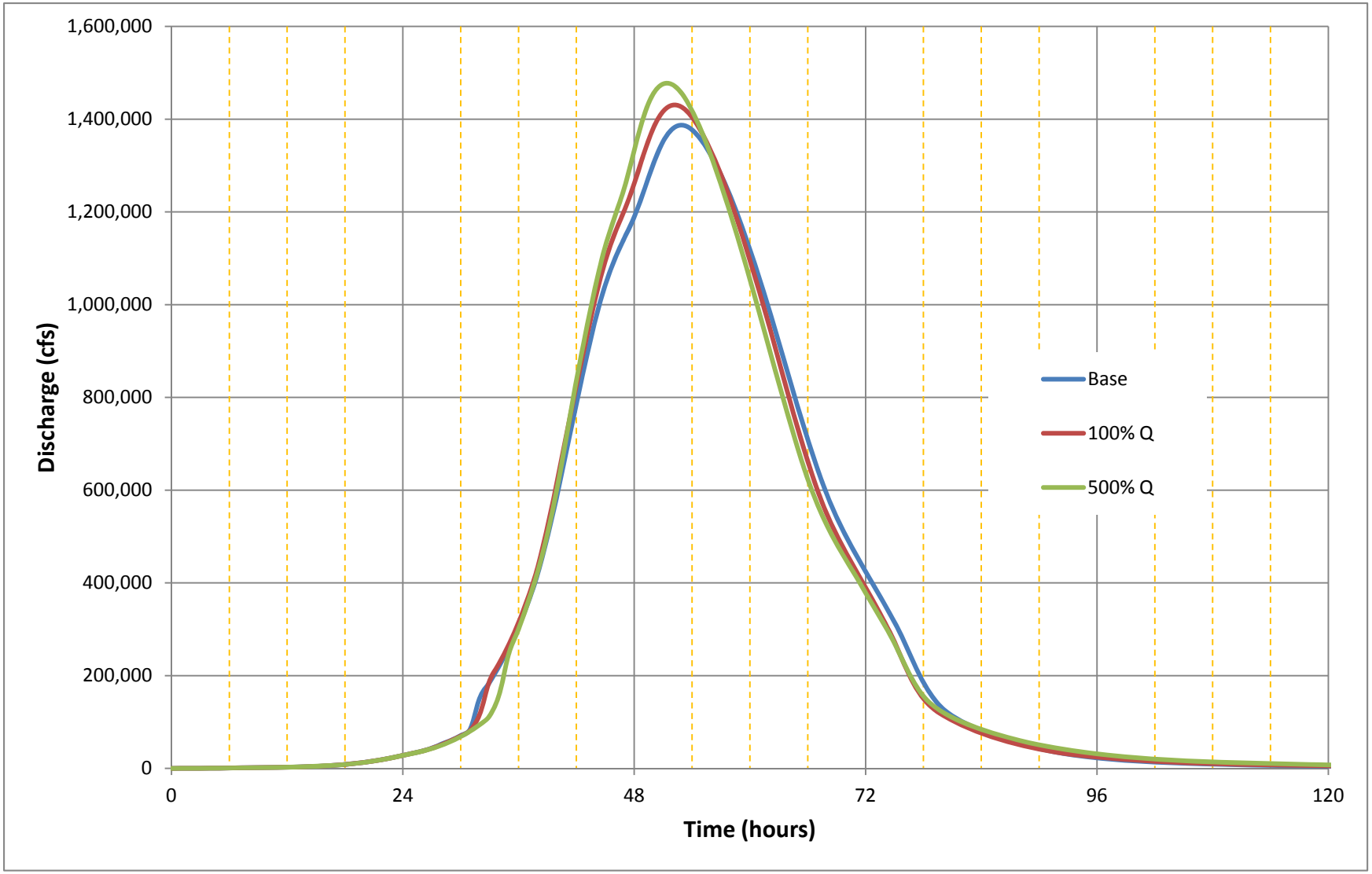

Figure 39. Comparison of Results

Chapter 5
Conclusions

This analysis focused on the changes to downstream hydraulic geometry based on an increase in dominant discharge driven by the ongoing changes of the earth's climate. This was accomplished using the Julien- Wargadalam (J-W) equations to parameterize the Muskingum-Cunge hydrologic routing method. In order to quantify the potential impacts of said changes, application was made to the Bluestone Dam watershed.

Results of the analysis showed three main findings. First, relative relationships between increasing dominant discharge and the resulting impacts to downstream hydraulic geometry was able to be determined by assuming constant grain size and sediment concentration. Second, the J-W equations proved to be able to accurately predict current channel geometry within the watershed. This allowed for the comparison to be made among changes to the downstream hydraulic geometry based on increased dominant discharge. Third, it was determined that as the dominant discharge of a river increases, the amount of flood wave attenuation which a river reach decreases. This reduction of attenuation is a product of the hydraulic geometry of the channel enlarging which reduces overbank storage and increases the hydraulic efficiency of the cross-section. The hydraulic properties used in the Muskingum-Cunge model are directly related to the physical cross-section through the use of the Manning's equation

As illustrated with the Bluestone Dam watershed, the decrease in attenuation did impact the resulting IDF hydrograph, however, due to the relative small percentage difference in results, was not determined to be a driving factor in the IDF development. As the knowledge surrounding climate change continues to expand, future flood developments may benefit from consideration of potential increased hydraulic efficiency throughout the drainage network of a watershed. All watersheds have varying non-linear relationships regarding the transformation of rainfall-runoff to channelized flow and the subsequent routing of floods through the watershed. Because of that, further testing would need to be completed to determine if a similar relationship calculated for the Bluestone Dam watershed holds true to other watersheds in different physiographic regions.

Chapter 6
References

Brunner, Gary W. *HEC-RAS River Analysis System: User's Manual*. Davis, CA: US Army Corps of Engineers, Hydrologic Engineering Center, 2010.

Brunner, Gary W. *HEC-RAS River Analysis System: Hydraulic Reference Manual*. Davis, CA: US Army Corps of Engineers, Hydrologic Engineering Center, 2010.

Garbrecht, Jürgen, and Gary W. Brunner. *A Muskingum-Cunge Channel Flow Routing Method for Drainage Networks*. Davis, CA: US Army Corps of Engineers, Hydrologic Engineering Center, 1991. Print. TP-135.

Global Climate Change Impacts in the United States, Thomas R. Karl, Jerry M. Melillo, and Thomas C. Peterson, (eds.). Cambridge University Press, 2009.

HEC, 2000. *HEC-HMS, Hydrologic Modeling System, Technical Reference Manual.* Hydrologic Engineering Center, U.S. Army Corps of Engineers, Davis, CA.

HEC, 2013. *HEC-HMS, Hydrologic Modeling System, User's Manual.* Hydrologic Engineering Center, U.S. Army Corps of Engineers, Davis, CA.

Julien, Pierre Y., and Jayamurni Wargadalam. "Closure to "Alluvial Channel Geometry: Theory and Applications." *Journal of Hydraulic Engineering J. Hydraulic Eng.* 122.12 (1996): 752.

Julien, Pierre Y. "Downstream Hydraulic Geometry of Alluvial Rivers." *Proc. IAHS Proceedings of the International Association of Hydrological Sciences* 367 (2015): 3-11.

Julien, Pierre Y. *River Mechanics*. Cambridge: Cambridge UP, 2002. Print.

Lee, Jong-Seok, and Pierre Y. Julien. "Downstream Hydraulic Geometry of Alluvial Channels." *Journal of Hydraulic Engineering J. Hydraulic Eng.* 132.12 (2006): 1347-352.

Lettenmaier, D., D. Major, L. Poff, and S. Running, 2008. Water Resources. In: *The effects of climate change on agriculture, land resources, water resources, and biodiversity.* A Report by the U.S. Climate Change Science Program and the subcommittee on Global change Research. Washington, DC., USA, 362 pp

M. A. Benson & D. M. Thomas (1966) A Definition of Dominant Discharge, International Association of Scientific Hydrology. Bulletin, 11:2, 76-80, DOI: 10.1080/02626666609493460

Melillo, Jerry M., Terese (T.C.) Richmond, and Gary W Yohe, Eds., 2014: Highlights of Climate Change Impacts in the United States: The Third National Climate Assessment. U.S. Global Change Research Program, 148 pp.

NOAA, 1978. *Probable Maximum Precipitation Estimates, United States East of the 105th Meridian, Hydrometeorological Report No. 51*, (HMR 51), National Weather Service, Washington D.C.

NOAA, 1982. *Application of Probable Maximum Precipitation Estimates, United States East of the 105th Meridian, Hydrometeorological Report No. 52*, (HMR 52), National Weather Service, Washington D.C.

SCS, 1986. *Urban Hydrology for Small Watersheds*, *Technical Release 55*, (TR-55), Soil Conservation Service, June 1986.

United States of America. Department of Defense. U.S. Army Corps of Engineers - Huntington District. *Water Control Manual for Bluestone Lake*. N.p.: n.p., 1994. Print

United States of America. Department of the Interior. Geological Survey. *The Hydraulic Geometry of Stream Channels and Some Physiographic Implications*. By Luna B. Leopold and Thomas Maddock. Washington: U.S. Govt. Print. Off., 1953. Print.

USACE, 1991. Inflow Design Floods for Dams and Reservoirs, Engineer Regulation 1110-8-2. U.S. Army Corps of Engineers, Washington, D.C.

USACE, 1994. Flood Runoff Analysis, Engineer Manual 1110-2-1417. U.S. Army Corps of Engineers, Washington, D.C.

Appendix A
Cross-Section Verification

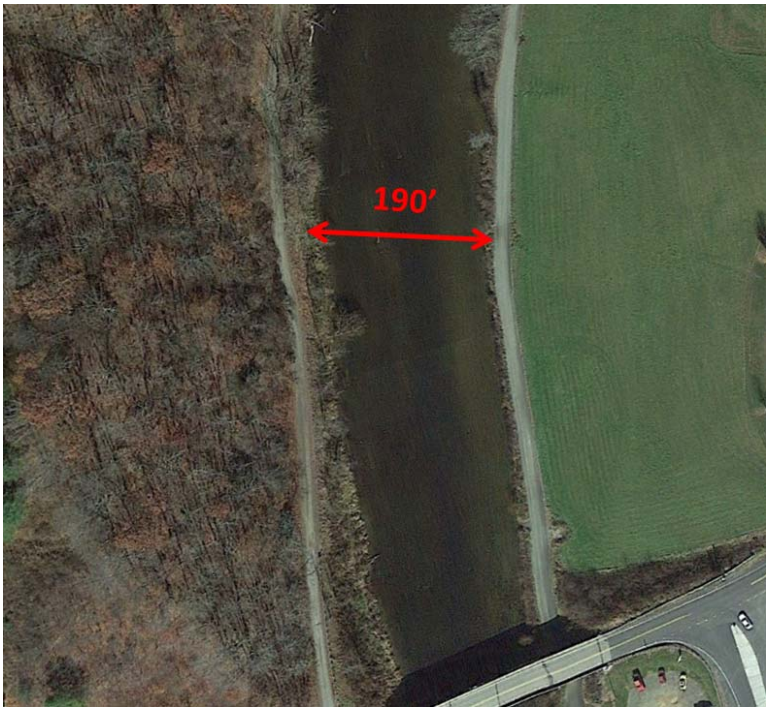

Figure 40. Current conditions near Jefferson, NC

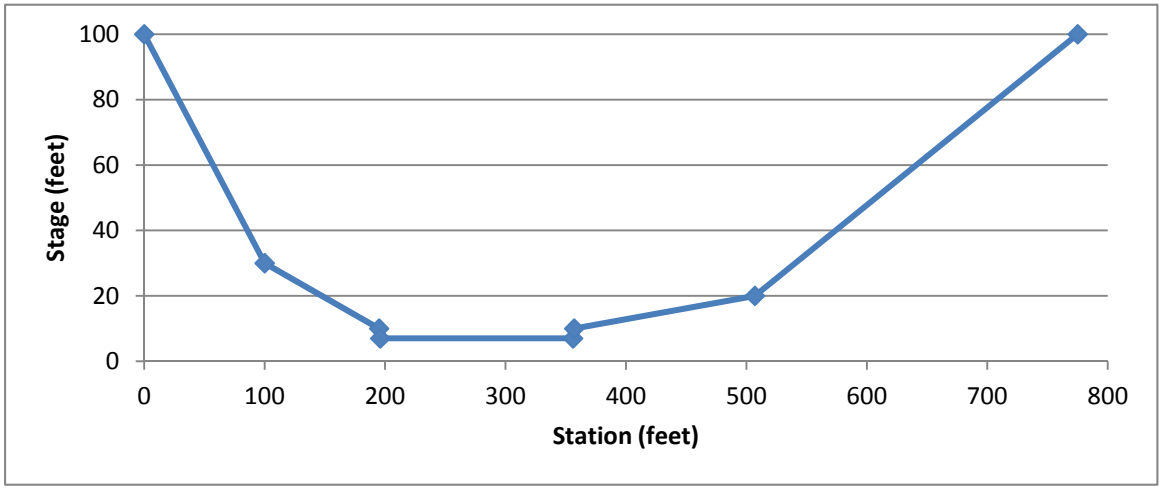

Figure 41. 8-point cross-section near Jefferson, NC

Table 15. Verification results for Jefferson, NC

Calculated Width (feet)	Measured Width (feet)	% Difference
162	190	15.9

Figure 42. Current conditions near Galax, VA

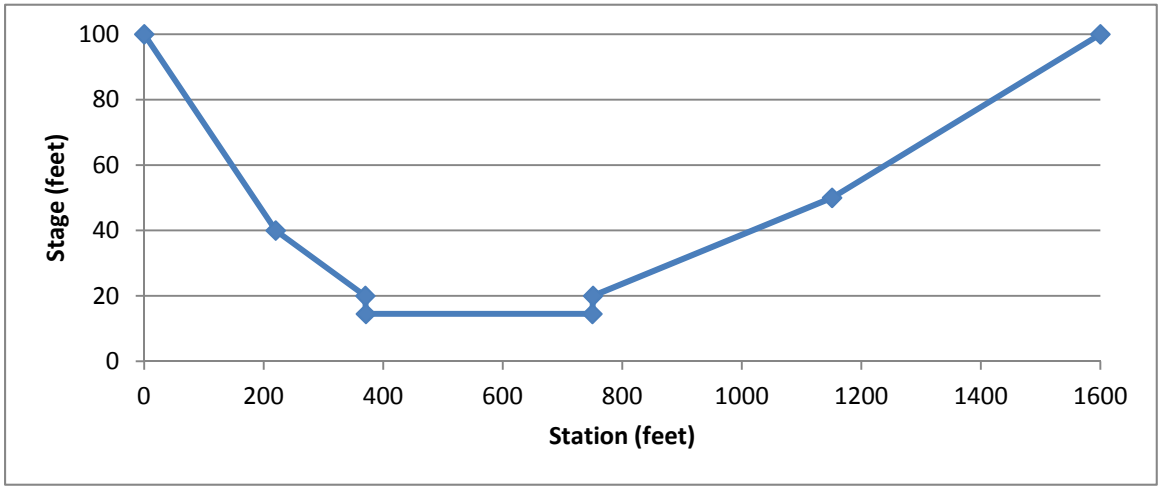

Figure 43. 8-point cross-section near Galax, VA

Table 16. Verification results for Galax, VA

Calculated Width (feet)	Measured Width (feet)	% Difference
381	480	23.0

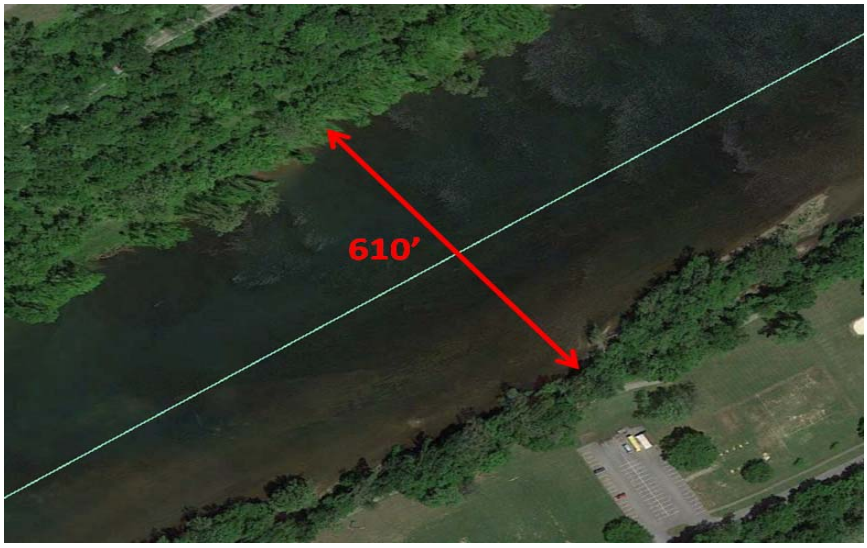

Figure 44. Current conditions near Radford, VA

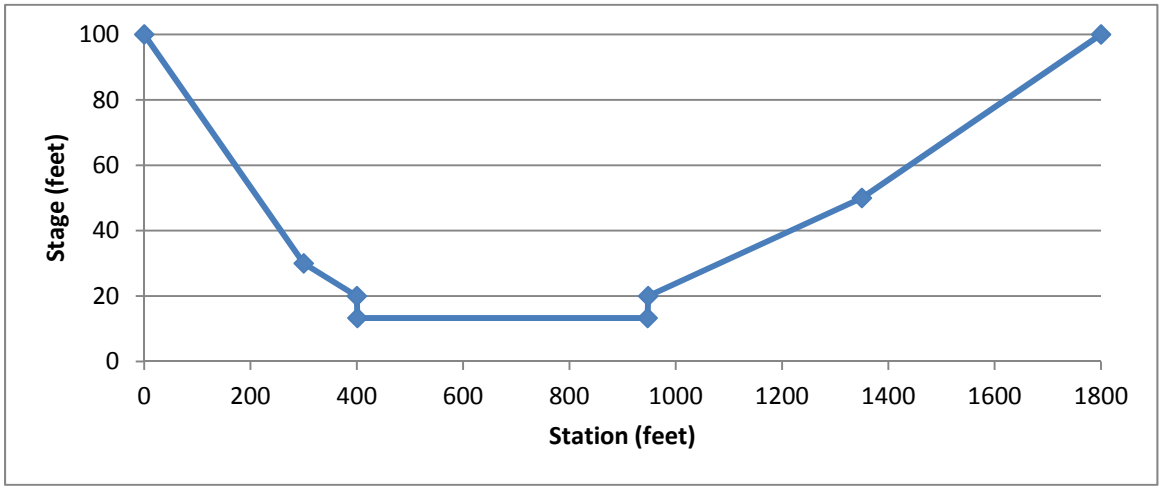

Figure 45. 8-point cross-section near Radford, VA

Table 17. Verification results for Radford, VA

Calculated Width (feet)	Measured Width (feet)	% Difference
548	610	10.7

Figure 46. Current conditions near Glen Lynn, VA

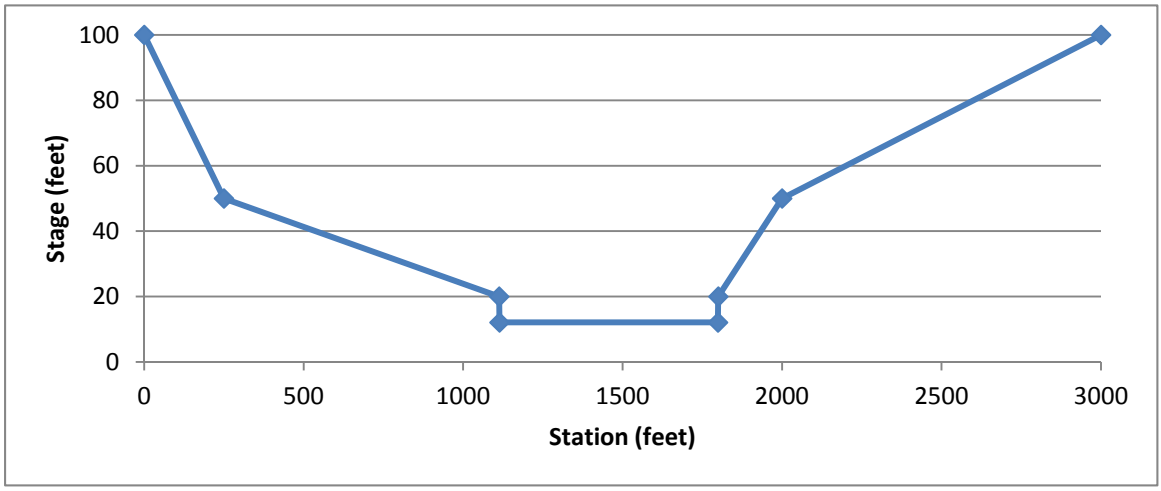

Figure 47. 8-point cross-section near Glen Lynn, VA

Table 18. Verification results for Glen Lynn, VA

Calculated Width (feet)	Measured Width (feet)	% Difference
687	660	4.0